2021

# The effect of onshore wind on wave overtopping of a vertical sea wall

Durbridge, S.

Durbridge, S. (2021) 'The effect of onshore wind on wave overtopping of a vertical sea wall',
The Plymouth Student Scientist, 14(2), pp. 311-355.
http://hdl.handle.net/10026.1/18508

The Plymouth Student Scientist
University of Plymouth

*The Plymouth Student Scientist, 2021, **14**, (2), 311-355*

# The effect of onshore wind on wave overtopping of a vertical sea wall

Sarah Durbridge

Project Advisor: Martyn *Hann*, School of Engineering, Computing and Mathematics (Faculty of Science and Engineering), University of Plymouth, Drake Circus, Plymouth, PL4 8AA

## Abstract

Strong winds can produce overtopping rates that are considerably higher than predicted by the EurOtop formulae, which do not make provision for wind. However, no detailed industry guidance exists about the quantification of those wind effects. Physical modelling tests (scale 1:21) investigated how the mean rate of overtopping changed with wave frequency under the influence of various wind speeds. The nature and quantity of overtopping was found to be strongly related to the frequency of the incident wave. The wind had a significant effect on the mean overtopping rate, with the most pronounced effect occurring when the overtopping was at its most impulsive.

Analysis showed that the wind had more influence than had been seen in other experiments, perhaps due to shallow water at the toe of the wall. Whilst the test results' specific values may not represent reality, it is suggested that their trends do. The findings suggest that design decisions that do not fully consider the wind's effect on overtopping might result in vertical sea walls that are too low to limit overtopping to acceptable rates when strong onshore winds influence it. These concerns are heightened if it is accepted that wind scaled according to Froude's law should be increased to make it compatible with real-life conditions.

**Keywords:** overtopping, vertical sea wall, onshore wind, EurOtop

## Introduction

It is accepted that climate change will cause sea levels to rise. A survey of 106 specialists (Horton et al., 2020) recently estimated that a rise of between 0.6 and 1.3 metres will have occurred by 2100, with an increase of between 1.7 and 5.6 metres being seen by 2300. Predictions made by the National Oceanic and Atmospheric Administration about global sea levels show that, on a low greenhouse gas emissions pathway, a minimum of 0.3 m rise is predicted by 2100; on the extreme emissions pathway, that rise could be as much as 2.5 m (Lindsey, 2021).

Rising sea levels will affect the use of coastlines around the world and the landmass available for habitation. In 2017 the United Nations reported that over 60% of the world's largest cities were in areas at risk, and approximately 10% of the world's population (600 million people) lived in coastal zones that were no more than 10 metres above sea level (United Nations, 2017). In 2020 the European Commission reported that over 200 million European citizens lived near the coast (European Commission, 2020). In the same year, the UK government reported that approximately 30% of people living in England and Wales reside within 10 km of the coast. Coastal regions contain a high proportion of land used for agriculture, manufacturing and the supply of energy. Further, the UK's coastline has both environmental and cultural heritage importance (Parliamentary Office of Science and Technology, 2020).

Climate change is also predicted to cause an increase in the frequency and severity of storms (Duarte et al., 2020), with wave conditions expected to change along European coasts (Bricheno and Wolf, 2018). This will mean that coastal defences will play an increasingly essential role in preventing the sea from passing on to the land. Overtopping of such structures can lead to flooding, property damage, infrastructure disruptions and the risk of physical harm (Williams et al., 2019). On average, up to five people die in the UK each year because of wave action, chiefly on sea walls or similar structures, and in 2005, 11 people lost their lives. Overtopping can also cause short or long-term damage to the coastal defence itself, leading to further breaching and flooding (Van der Meer et al., 2018).

Whilst there are many different types of coastal defences, this paper focusses on vertical sea walls and, specifically, the extent to which onshore wind affects wave overtopping. Strong winds during storms can produce average and maximum overtopping discharges at these structures that are considerably higher than those predicted by empirical formulae, which do not include the potential impact of wind. However, no detailed guidance exists about how those wind effects should be quantified. As weather conditions and water levels become more challenging, the probability of sea walls being overtopped will increase and the need for such guidance will become increasingly pressing. Engineers will have to determine whether existing sea defences remain fit for purpose or whether they should be retro-fitted with add-ons that improve their resilience (Dong et al., 2020). Also, the approach to designing new structures may need to change.

The sections below set out the paper's objectives, contain a literature review and detail the method used for the physical modelling tests. Later sections of the paper explain how overtopping predictions were obtained using the EurOtop formulae (Van

der Meer et al., 2018) and an artificial neural network tool (H R Wallingford, 2019) and discuss the results. The final sections contain conclusions and recommendations.

## Objectives

This paper's objectives are to:

- establish the industry's current understanding of how wind affects overtopping of vertical sea walls;
- review the issues surrounding the simultaneous scaling of wind and waves;
- use physical modelling tests to investigate how the mean rate of overtopping at a vertical sea wall changes with differing (peak) frequencies of regular and irregular waves under the influence of wind of varying strengths;
- analyse the collected data to determine the effect of onshore wind on the mean rate of overtopping; and
- investigate the application of the experiment's results to real-life structures.

In satisfying the above objectives, this paper addresses the following key questions:

(i) Can the results obtained during the physical modelling tests be relied on given the issues surrounding the simultaneous scaling of wind and waves?
(ii) Did the results from the physical modelling tests concur with the EurOtop manual (Van der Meer et al., 2018)'s limited guidance about the effect wind has on overtopping?
(iii) Does it matter that wind effects are not accounted for within the EurOtop formulae?

## Literature review

### Sea walls

Sea walls are popular in many European countries (Allsop et al., 2005) and human-made defences, predominantly sea walls, protect over 20% of the English coast (approximately 860 km) (H R Wallingford Ltd, 1999). Many of those walls were built by the Victorians to provide promenades at seaside resorts. Many more were constructed during the 1930s by unemployment relief schemes, even though they often caused problems with erosion, either close to their location or further along the shore (Reeve et al., 2012). Nowadays, sea walls are generally constructed along urban frontages to reduce the impact of tides and waves (Van der Meer et al., 2018). They are expensive to construct but protect people, property, land and economic activities from erosion, flooding (Environment Agency, 2015) and local overtopping hazards (Allsop et al., 2005).

Whilst sea walls can be constructed from different materials with varying profiles (Environment Agency, 2015), this paper focusses on impermeable vertical sea walls. Such walls are subjected continuously to wave action. If waves break directly on them, they can overtop violently and suddenly, with localised high impact pressures (Van der Meer et al., 2018).

## Overtopping of vertical sea walls

There are two principal types of overtopping: green and impulsive (Van der Meer et al., 2018). Both types can cause significant water volumes to pass over the wall's crest, but in very different ways. Green overtopping occurs when a continuous sheet of water runs up and over the wall's crest. Impulsive overtopping occurs where some of the waves break on to the wall, sending vertical plumes of highly aerated water over the crest. The waves that break against the wall can produce short-duration forces up to 40 times larger than seen in non-impulsive conditions. It is also possible for water to pass over the crest of a vertical wall as spray, caused by the wind's action on the waves. Whilst this can cause visibility hazards behind the sea wall, it does not contribute significantly to overtopping rates (Van der Meer et al., 2018).

The two most significant measures of overtopping are the mean discharge per linear metre of wall width ('q') (in l or $m^3$/s per m) and the maximum volume of discharge caused by a single overtopping wave ('$V_{max}$') (in l or $m^3$ per wave per m width). Overtopping cannot be fully described by q alone because it is a complex phenomenon, random in volume, time and location (Altomare et al., 2020). Depending on the amount of overtopping, $V_{max}$ will be 100 to 1000 times larger than q. Whilst many small overtopping waves can produce the same q as a few large waves in a rough sea, more prolonged storms and rougher seas will generally produce larger $V_{max}$ values. From a design perspective, it is the largest waves, at or near the $V_{max}$ value that are likely to cause the most damage (Van der Meer et al., 2018).

$V_{max}$ and q are both affected by structural and hydraulic parameters. Structural parameters include the wall's geometry, crest width and crest level. Hydraulic parameters include the water depth at the toe of the structure, the wave period, the direction of the incident waves and the significant wave height (Van der Meer et al., 2018).

Research over the last few years has found that tolerable overtopping depends very strongly on $V_{max}$ and that $V_{max}$ is strongly related to the height of the wave causing the overtopping. A single large wave breaking against a sea wall with a large crest freeboard can cause many $m^3$ of overtopping, whereas waves with small wave heights will only produce small overtopping volumes. This research has led to a change in the EurOtop manual's guidance, which now states that q should be coupled to a wave height causing that discharge, and that tolerable overtopping limits should be based on $V_{max}$, not just q (Van der Meer et al., 2018).

## Methods for assessing and predicting overtopping

Overtopping is an essential factor in the design of coastal structures (den Bieman et al., 2020) and, as a result, is a well-researched area of coastal engineering. Whilst measurements during storms are scarce and difficult to obtain (Oliveira et al., 2020), and mean overtopping measurements taken in the field are rare (Pullen et al., 2009), many investigations have been carried out using scaled physical models, empirical models, numerical modelling and artificial neural networks (Pullen et al., 2018). The following sections review these approaches (except numerical modelling, which is not relevant to this paper).

Physical modelling

Hughes (1993) defines a physical model as "…a physical system reproduced (usually at a reduced size) so that the major dominant forces acting on the system are represented in the model in correct proportion to the actual physical system". Benefits of physical modelling include that scaled experiments are cheaper than field measurements, and the data is easier to collect. There is a higher degree of experimental control than in the field, and the observer can see results in the making. Also, there is no need to make the simplifying assumptions that numerical models require. Disadvantages principally relate to scale and laboratory effects, which are discussed further below.

Typical scaling for short wave physical models for 2d wave transformation is between 1:10 and 1:50 (Hughes, 1993). The physical modelling tests to which this paper relates used a scale of 1:21.

Obtaining the correct scale determination is fundamental to the success of an experiment. The Froude law and the Reynolds number are both significant scaling criteria. The former assumes that gravity is the dominant force balancing inertial forces, and ignores other forces, including viscosity, elasticity and surface tension. The latter provides the relationship between inertial and viscous forces (Hughes, 1993). Whilst Van der Meer et al. (2018) stated that physical modelling results should only be considered reliable if both these rules have been followed, this is physically impossible to achieve. Therefore, within the coastal engineering industry, the Froude law is used to scale most models, and Hughes (1993) recommends it for vertical wall structures.

The incompatibility of Froude's law and the Reynolds number means that scale effects in physical modelling tests are inevitable. The significance of these effects has been the subject of several research papers, with conflicting conclusions. Kerpen et al. (2020) suggested that as viscosity, elasticity and surface tension could affect the nature of wave breaking and resulting overtopping volumes, results could be inaccurate because of incorrect scaling of those factors. Similarly, Van der Meer et al. (2018) asserted that surface tension could be significant in very small-scale models when wave periods were shorter than 0.35 seconds, the water depth was less than 2 cm, or the significant wave height was less than 5 cm. However, as part of the VOWS (Violent Overtopping of Waves at Seawalls) research project, Pearson et al. (2002) conducted over 30 tests, each with approximately 1000 irregular waves. They found that despite the highly aerated flow of the impulsive overtopping jet, large and small scale results were in close agreement, both for q and $V_{max}$. This conclusion has been supported by Pullen et al. (2009), who, as part of the CLASH[1] project, compared measurements of wave overtopping at Samphire Hoe's vertical sea wall with results from 2D and 3D physical model testing. This study determined that it was not necessary to consider scale effects when comparing field and

[1] Crest Level Assessment of Coastal Structures by Full-scale Monitoring, Neural Network Prediction and Hazard Analysis on Permissible Wave Overtopping

laboratory results for vertical sea walls. The only adjustment required was for the effect of wind (see further below).

Laboratory effects arise from differences between prototype and model responses caused by limitations of the equipment. Examples include the incorrect reproduction of the prototype's geometry in the scaled model, different equipment used to collect data from the model and the prototype, and wave flume boundaries, which do not mimic an open sea (Van der Meer et al., 2018). Another common issue is the reflection of wave energy by the wave paddle. In real life, waves reflected by the sea wall would travel out to the ocean, but in the flume, they can get reflected by the paddle back towards the model (Hughes, 1993). To combat this problem, paddles have active wave absorption, but this is unlikely to work perfectly. The build-up of reflected wave energy was considered during the physical modelling tests and found to be relevant at certain frequencies (see the "Impact of run time" subsection in the Results section below).

Due to the number of parameters that influence overtopping, physical models often produce more accurate results than empirical or numerical models (Van der Meer et al., 2018). However, the overtopping process is so complex that it is still not fully understood, and, therefore, research continues. For example, in a study limited to a non-influencing foreshore and intermediate water depth, Kerpen et al. (2020) attempted to develop a more realistic physical modelling test by including a changing water level and varying wave steepness. Whilst they found that the existing EurOtop formulae (Van der Meer et al., 2018) covered the dynamic water level, the variation in wave steepness created uncertainties of up to a factor of two. Kerpen et al. recommended further tests in shallow water, and that wave generation tests should be adjusted to compensate for reflected waves in changing water levels.

Williams et al. (2019) used physical modelling to quantify the uncertainty caused when generating multiple wave time series from the same spectrum. The study found that it was not easy to remove the standard deviation caused by laboratory effects (approximately 1%). The study further found that the standard deviation in q caused by the seeding variability increased significantly as the dimensionless freeboard (R*) increased: the lower the overtopping, the higher the variation. The study recommended accounting for this variability factor by repeating tests in the region of $R^* > 2$ to estimate the range of the dimensionless overtopping rate. A minimum of 20 repetitions was recommended for overtopping with a probability of less than 10%. For higher overtopping probabilities, this recommendation was reduced to a minimum of 10 repetitions.

Empirical models

Empirical models use dimensionless equations to relate structure and wave parameters to response parameters. The equations are adjusted both in respect of their form and coefficients to reproduce overtopping results derived from either physical modelling or field data (Van der Meer et al., 2018), and most are based on data contained in the CLASH database (Van Gent et al., 2007). The formulae generally have specific applicability limits and therefore need to be used with caution.

EurOtop manual

The EurOtop manual (Van der Meer et al., 2018) aims to enable engineers to establish tolerable overtopping rates and volumes for a structure and then use its formulae to make sure that those discharges are not exceeded. It is accepted as an international best practice tool (Environment Agency, 2020) and its semi-empirical formulae (updated by the second edition) (Van der Meer et al., 2018) are commonly used by coastal engineers (Altomare et al., 2020).

The manual's formulae for predicting overtopping at a vertical sea wall were applied to the irregular waves selected for the physical modelling tests (see further below). Also, the manual's design and assessment formulae, which include a partial safety factor, were considered when determining whether the effect of wind on overtopping is adequately covered (see further below). The formulae depend on whether there is an influencing foreshore, a significant mound in front of the structure's toe or a likelihood of impulsive overtopping. The size of the relative freeboard is also a factor. The formulae produce a value for a non-dimensional version of the mean overtopping discharge ($q/\sqrt{(gH_{m0}^3)}$), which is easier to measure in a flume test than wave by wave overtopping (Van der Meer et al., 2018).

The formulae have accuracy limitations due to the inherent scatter within overtopping data. Van der Meer et al. (2018) advise that calculated overtopping rates will only be, at best, within a factor of one to three of the actual overtopping, and that the largest deviations will occur with low overtopping rates. Also, the manual states that its empirical methods based on scaled tests using generic structures will not produce results that are as accurate as tests based on structure-specific models. The EurOtop manual only gives general guidance about the effect of wind on overtopping rates. That guidance is considered in detail below.

Artificial Neural Networks

Artificial neural networks (ANNs) have been developed to predict overtopping in situations that are not well suited to empirical formulae, including complicated geometrical structures and variable wave conditions (Zanuttigh et al., 2014). They can provide a good compromise between time efficiency and accuracy, and produce nearly instantaneous results, thereby giving them advantages over numerical models (Formentin et al., 2017).

When the EurOtop manual (Van der Meer et al., 2018) was published, the EurOtop ANN (Zanuttigh et al., 2016; Formentin et al., 2017) was also released. This tool contains over 13,000 overtopping tests and can predict q and the 90% confidence band for many structures. Van der Meer et al. (2018) suggest that, for very specific structure shapes, the ANN should predict overtopping at least as accurately as the EurOtop manual's empirical formulae, and that it is better equipped to deal with low overtopping rates than its forerunner (the CLASH database).

In 2020, the government released a new generic meta-modelling overtopping model named Bayonet GPE2 (Environment Agency, 2020). Its creators, Pullen et al. (2018), have asserted that this model addresses two principal issues within the CLASH and EurOtop ANNs. Firstly, those models do not account for uncertainty within themselves (it is dealt with by confidence interval estimates), leading to underestimation. Secondly, they assume that each parameter is independent, which might mean that users unwittingly rely on predictions outside of the models' range. The Bayonet GPE model has been used to predict overtopping for the irregular wave series selected for the physical modelling tests (see further below).

## The effect of wind on the overtopping of vertical sea walls

Wind can affect overtopping processes and the resulting discharges by blowing up-rushing water over the wall's crest, thereby increasing both the wave by wave overtopping volume and q (Van der Meer et al., 2018). It can also change the shape of the wave crest incident to the structure, potentially changing the wave interaction regime with the wall (Pullen et al., 2009).

## Methods for assessing the effect of wind

Whilst the process of overtopping is a well-researched area of coastal engineering, the same is not true for the effects of wind on overtopping. As stated above, no detailed guidance exists within the EurOtop manual. There have only been a couple of field studies, both of which struggled when assessing scale effects (Pullen et al., 2009), and only a limited number of research papers have been published on the subject. The following sections review the available information.

### Physical modelling

Scaling is a fundamental issue in modelling wind, especially concerning air-spray mixtures, where droplet size, surface tension and viscosity are the same size for the model as for the prototype (Pullen et al., 2009). De Waal et al. (1996) commented that the wind's shear velocity should be to scale because the waveform is influenced by the shear stress of the wind acting on the water surface. Also, potential scale effects arise from the drop transport capacity of the wind not being known.

When an overtopping discharge breaks up into spray, this process depends upon surface tension effects, which should be scaled using Weber's equation. However, it is not possible to simultaneously satisfy Weber's and Froude's scaling laws (Pullen et al., 2009). For this reason, it has been suggested that wind scaled according to

[2] Based on a Bayesian overtopping model and Gaussian process elimination techniques

Froude's law should be increased during physical modelling tests if it is to produce similar results to those seen in the field. Whilst their study related to a rubble mound breakwater, Jensen and Sorensen (1979) found that model wind speeds needed to be more than double that given by Froude scaling to make them comparable to field conditions. Muzik and Kirby (1991) compared field data from a Canadian island with results obtained using a 1:30 3D Froude scaled model and concluded that the multiplication factor should be approximately 3.75. Yamashiro et al. (2004) compared field observations of wave overtopping with results obtained using a 2D model test at a scale of 1:45. They concluded that values of q were equivalent in the field and the laboratory when wind velocity in the laboratory was 1/3rd of that in the field.

The production of the effects of wind is another significant issue in physical modelling tests. Generally, experiments have used either a large fan (as for the physical modelling tests upon which this paper is based) or a paddle wheel. However, neither of these methods are ideal. Van der Meer et al. (2018) stated that there is no reliable way to relate the wind from a fan to real-life wind conditions. Also, wind in real life cannot push forward the large volumes of up-rushing water that occurs with a paddle, meaning that any suggested increase factors in that scenario will be over-estimated. As stated above, only a few physical modelling experiments have investigated the effect of wind on overtopping. These are reviewed in detail below.

Iwagaki et al. (1966) used an enclosed 40 m wind tunnel and a high-speed electric fan blower to investigate the relationship shown in Figure 1 below. They compared the rate of wave overtopping ($2\pi Q/H_0L_0$) with the dimensionless wind velocity ($V/\sqrt{(gH_0)}$), using relative wall height ($H_c/H_0$) for each relativee water depth ($h/L_0$) and two values for wave steepness ($H_0/L_0$) of 0.01 and 0.02.

$$2\pi Q/H_0L_0 = F(H_c/L_o, H_c/H_0, h/L_0, V/\sqrt{gH_0})$$

where Q = Wave overtopping volume per wave period, $H_0$ = Wave height, $L_0$ = Wavelength,

$H_c$ = Crest height of sea wall, h = Water depth at toe of sea wall, V = wind velocity and g = acceleration due to gravity

**Figure 1:** Relationship between wave overtopping and wind (Iwagaki et al, 1966)

Iwagaki et al. concluded that the wind's effect varied considerably with the relative water depth at the toe of the sea wall, even when wave steepness was constant. They found that when the incident waves did not break in front of the sea wall, overtopping suddenly increased when the wind reached a certain velocity: for a wave steepness of 0.01, this occurred when $V/\sqrt{(gH_0)}$ reached 6 to 7; for a wave steepness of 0.02, the relevant value of $V/\sqrt{(gH_0)}$ was 3 to 5. For waves that broke just in front of the sea wall, causing water to rise high over the wall, they asserted that there was a complicated relationship between $V/\sqrt{(gH_0)}$ and wave steepness: when $V/\sqrt{(gH_0)}$

had a value of 2 to 3, the overtopping rate was constant, which could have been due to the waves becoming fine drops of water, almost all of which overtopped the wall; when $V/\sqrt{(gH_0)}$ was 5 to 7, the overtopping rate decreased, perhaps because the water drops were so fine that they could not be collected in the overtopping tanks.

In the 1990s, the Coastal Engineering Research Centre (CERC) of the US Army Engineer Waterways Experiment Station and Texas A&M University ran a joint project to assess the effect of wind on wave run-up and overtopping. Ward et al. (1994) concluded that overtopping estimates that did not include wind effects would be too low because applying wind to the tested wave conditions had produced large increases in overtopping. In a study that does not mention the scale of the physical modelling tests, Ward et al. (1996) found that a wind speed at scale of 6.5 m/s had little effect on overtopping, but that wind speeds of 12 m/s or more greatly increased q. They also concluded that the mechanical reproduction of a combined wind/wave effect would not produce the same results as wind acting directly on a wave because it would not reflect the changes that the wind made to the wave profile. They made a further general observation that the increase in q due to wind was large when the discharge rate was low, but that the wind's effect decreased as q increased. This observation has since been supported by Pullen et al. (2009).

De Waal et al. (1996) used a 1:20 wave flume experiment, with a rotating paddle wheel, to assess the maximum influence wind could have on q. Figure 2 below shows the "spray transport factor" ($W_s$) used to describe the difference between the discharge that would travel over the wall's crest with and without the influence of wind.

$$W_s = \frac{Q_{\text{with spray transport}}}{Q_{\text{without spray transport}}}$$

$Q$ = mean overtopping discharge = $q/\sqrt{(gH_{os}^3)}$

$q$ = average overtopping discharge ($m^3/s$ per m)

$g$ = acceleration due to gravity = 9.81 $m/s^2$

**Figure 2**: Equation for spray transport factor (de Waal et al., 1996)

Whilst de Waal et al. found that q was greater for all tests with spray transport than those without, the maximum value of $W_s$ was only about 3.2, occurring for breaking or broken waves. They concluded that this factor was of the same order as the inherent scatter seen within overtopping data from other investigations. They further stated that the assessment of the relationship between the actual wind speed and the additional portion of transported breaker spray was not very useful. They suggested that the wind's effect on the wave height at the structure could be accounted for by adjusting the significant wave height in the empirical overtopping formulae. They recommended further investigations, stating that there were still unknowns that could not be computed, namely the shape and breaker type at the structure, and the influence of wave reflection from the wall on the wind's deformation of the wave. The second of these unknowns is considered below.

Research papers published by de Rouck et al. (2005) and Pullen et al. (2009) suggested a wind adjustment factor ($f_{wind}$) dependent upon q that could be applied to small overtopping rates of between 0.01 and 10 l/s per m. Pullen et al. (2009) explained that this was not a scale effect adjustment in that laboratory results might differ from field data, rather it allowed lower q values to be factored up in the presence of strong onshore winds. De Rouck et al. (2005) commented that this distinction was important because no scale effects for vertical structures had been observed. Figure 3 below gives the formula for $f_{wind}$ and shows that the adjustment factor reaches a maximum of four for q of up to 0.01 l/s per m and a minimum of one for q exceeding 10 l/s per m. Whilst the range of wind speeds to which this adjustment factor might apply was not specified (and interestingly, $f_{wind}$ does not vary with wind speed), Pullen et al. referred to a storm during field observations with gale force winds that were strong enough to make it difficult to walk, and laboratory test wind speeds (not scaled up to prototype) of between 15 and 28 m/s. These speeds are much higher than those applied to the irregular waves during the physical modelling tests to which this paper relates (maximum speed at scale was 7 m/s).

$f_{wind} = 4.0$ for $q_{ss} < 1x10^{-5}$ $m^3/s/m$

$f_{wind} = 1.0 + 3\left(\frac{-logqss-2}{3}\right)^3$ for $q_{ss} < 1x10^{-2}$ $m^3/s/m$

$f_{wind} = 1.0$ for $q_{ss} \geq 1x10^{-2}$ $m^3/s/m$

$q_{ss}$ = small scale model overtopping result (already scaled up to prototype scale) or a prediction by the CLASH neural network or similar

**Figure 3:** Equation for wind factor (de Rouck et al, 2005)

Murakami et al. (2019) commented that wind velocity and direction are not considered when sea walls are designed, but that it is important to understand the effect of wind on overtopping if safe land use is to be achieved behind a sea wall. For this reason, they conducted a test flume experiment to investigate the effect of wind velocity on individual wave overtopping at both a vertical and a flared sea wall. The study found that wind increased the individual wave overtopping volumes for each wave period. Also, there was a dependency between the wind velocity's influence and the wave period: shorter wave periods produced a larger difference between the no wind and wind applied overtopping than longer wave periods. To enable q under a wind condition to be estimated, Murakami et al. proposed the equations for $V_r$ (the ratio of the wave overtopping quantity with wind to the quantity without wind) and α (the wave overtopping parameter), shown in Figure 4 below.

$V_r = Exp\ (\alpha * (U/\sqrt{(gh_o)}))$

$\alpha = \left(\frac{H_{1/3}}{h_c}\right)\left(\frac{L_o}{h_c}\right) + b$

U = wind velocity (m/s)

g = acceleration due to gravity = 9.81 $m/s^2$

$h_o$ = offshore water depth (m)

a and b = linear constants

$H_{1/3}$ = significant wave height (m)

$h_c$ = crown height (m)

$L_o$ = offshore wavelength (m)

**Figure 4**: $V_r$ and α equations (Murakami et al., 2019)

In deriving the equation for the wave overtopping parameter, Murakami et al. took account of parameters affecting q, namely the wall crown height, the incident wave height, and the incident wave period. They stated that, for the vertical structure, α decreased with the model parameter $((H_{1/3}/h_c)*(L_o/h_c))$, meaning that the effect of the wind velocity on $V_r$ decreased as the model parameter increased. A good correlation was found between the measured and calculated values for the vertical sea wall.

The findings from the above research papers are discussed further when considering the results of the physical modelling tests.

EurOtop manual

Van der Meer et al. (2018) did not model wind when deriving the overtopping formulae for the EurOtop manual, and only limited guidance is given in the manual about wind effects. For green overtopping, it advises that onshore winds do not have any real effect on large values of q, but that q of less than 1 l/s per m might be increased by up to four times under strong winds. Whilst the term “strong winds” is not defined, Van der Meer et al. (2018) suggest that this increase would be because wave overtopping at this level is partly spray, so the droplets could be blown inshore by the wind. The manual further states that, for prototypes, the lowest discharges are likely to be the most influenced.

The manual states that wind effects could increase as overtopping becomes more impulsive. However, when q is less than a few l/s per m, whilst there might be a wind effect, this is likely to be subsumed within the 90% confidence band reflecting the prediction’s reliability (Van der Meer et al., 2018).

The accuracy of this guidance is discussed below.

## Method

### Initial design and scaling

The design of the physical modelling tests was influenced by Case Study 12 within the EurOtop manual, based on the vertical sea wall at Samphire Hoe, Dover (Van

der Meer et al., 2018). That wall has a relatively high freeboard. There is an influencing foreshore and impulsive wave overtopping conditions prevail.

Froude's law was used to scale the model (Hughes, 1993). Figure 5 below shows its principal dimensions, based on a scale of 1:21.

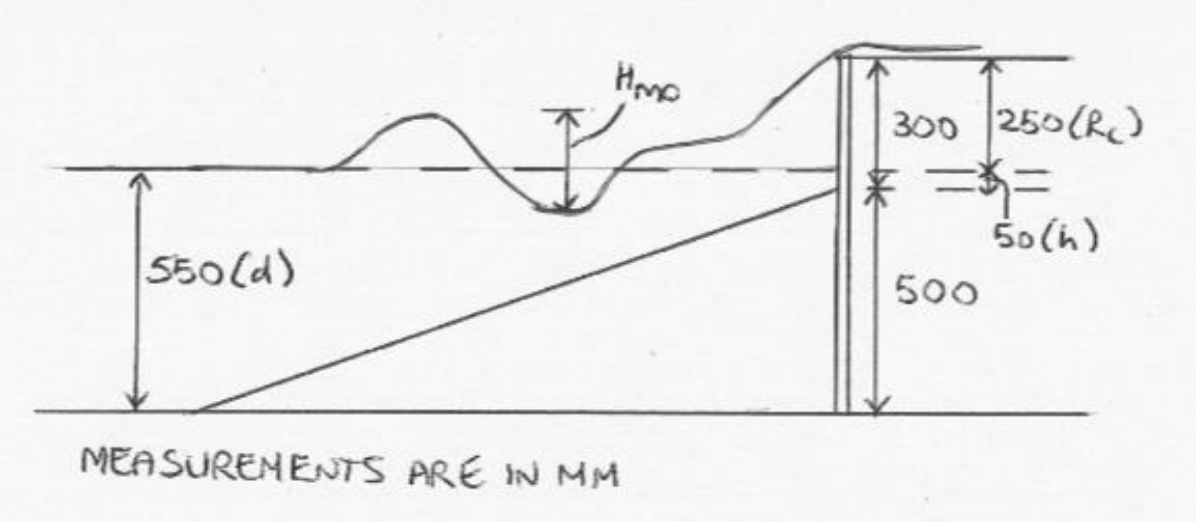


**Figure 5:** Principal model dimensions

## Equipment

Testing was carried out using a wave flume at Plymouth University's COAST laboratory. The glass-sided flume was horizontal, 35 m long, 0.65 m wide and approximately 1.1 m deep. It had a piston-type wave generator paddle with active absorption, producing waves normal to the model of the sea wall. Figure 6 below shows the key elements of the setup.

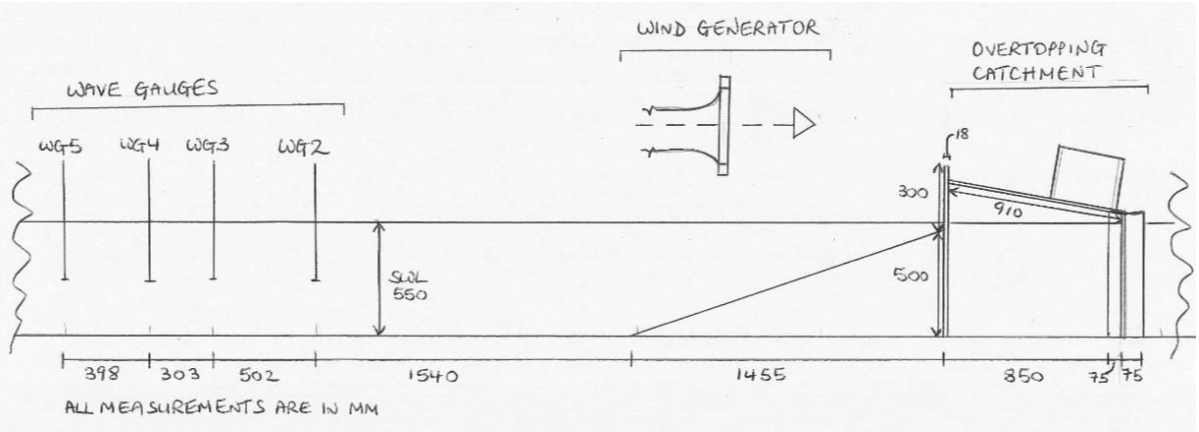


**Figure 6**: Physical modelling test setup

The water level in the flume was set at 0.55 m. This level was checked twice a day and topped up as required. Generally, during a day, the tank's level dropped by 5 mm, most likely because of water lost from larger overtopping events. When the flume was not used for two days, the tank's level dropped by 10 mm, most likely because of evaporation.

Figure 7 below shows the flume's wave paddle. Figure 8 below shows the setup of the wooden foreshore slope and vertical wall. A standard procedure was used to capture overtopping (Williams et al., 2019). A wooden chute was placed behind the structure's crest, which was the width of the flume, 0.91 m long, and flowed into the overtopping collection container (see Figure 10 below). That container was constructed from a 0.15 m diameter plastic pipe of height 0.56 m. The overtopping was measured by a resistance type gauge ('the depth gauge'), and an electric pump was used to remove the collected water when required.

**Figure 7:** Wave paddle

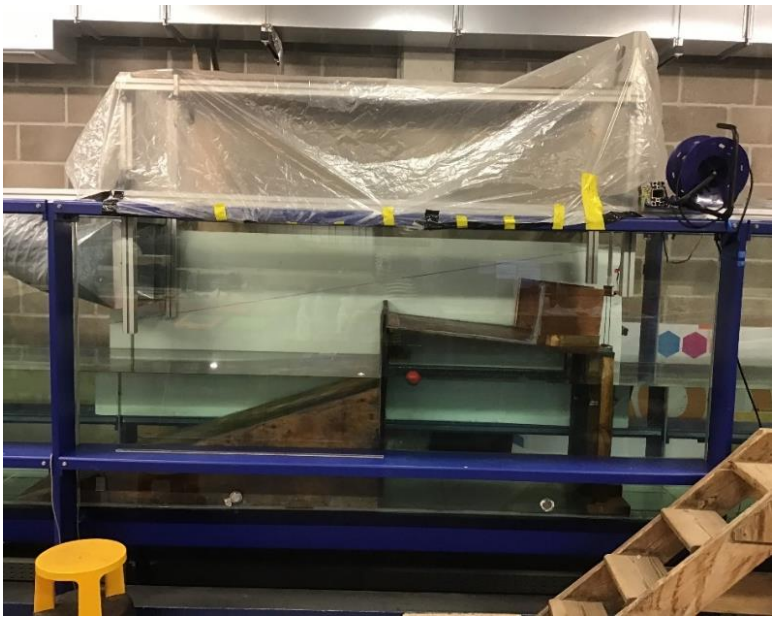

**Figure 8:** Vertical wall, slope and overtopping runoff set-up

Figure 9 shows the wind generator (with its flue and outlet) that was used to direct wind towards the vertical wall. The outlet's base was placed level with the top of the vertical wall and 1.05 m from the wall. This location was chosen in preference to further down the flume so that the wind would not affect the propagation of the incident waves but would assist in pushing the overtopping discharge over the wall's crest (Pullen et al., 2009). The cover above the vertical wall and run-off area (see Figure 8) was constructed to prevent too much water from being lost from larger overtopping events (de Waal et al., 1996), which could have affected the results' validity and caused a health and safety hazard to laboratory users. It comprised a metal frame with wooden boards placed on top, with thick plastic sheeting draped down both sides of the flume but kept shorter and taped into position on the operator's side of the tank so that it did not obscure the tests.

**Figure 9:** Wind generator and wave gauges

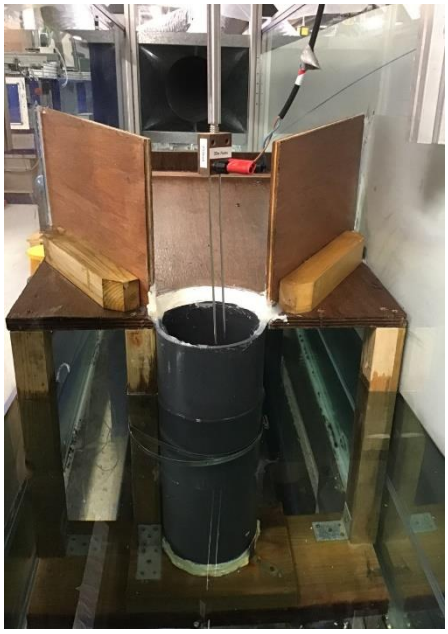

**Figure 10:** Overtopping container

Four resistance type wave gauges were placed between the wave paddle and the vertical wall to measure the free surface of the water. Figs.6 and 9 above show their locations relative to the wall and foreshore slope. The distance between the front of the wave paddle (in its powered-up position) and wave gauge 5 was 19.96 m. Wave gauge 2 was located as close to the end of the foreshore slope as possible, considering the fixtures for the wind generator outlet. All gauges were placed at approximately mid-water depth.

### Wave gauge and depth gauge calibration

The four wave gauges were calibrated daily using the standard laboratory procedure. Calibration of the depth gauge occurred three times during testing. The overtopping container was emptied, one litre of water was added, and the container's water level was allowed to settle. Water was then added in one-litre steps until the container was full. Using the data collected on 11 November 2020 as an example, the test length was plotted against the recorded voltage (see Figure 11 below). That plot was used to determine the average voltage at each litre step, which was then plotted against water volume. Figure 12 below shows this data for each of the calibrations. The gradient coefficients of the best fit lines were applied as voltage multipliers when the results were analysed using MATLAB.

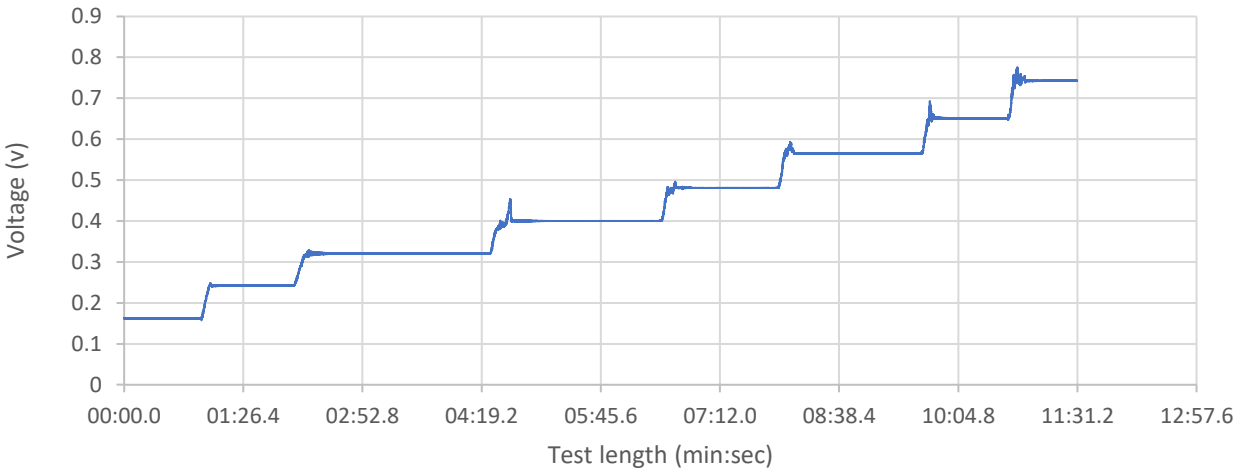


**Figure 11:** Depth gauge calibration – 11 November 2020

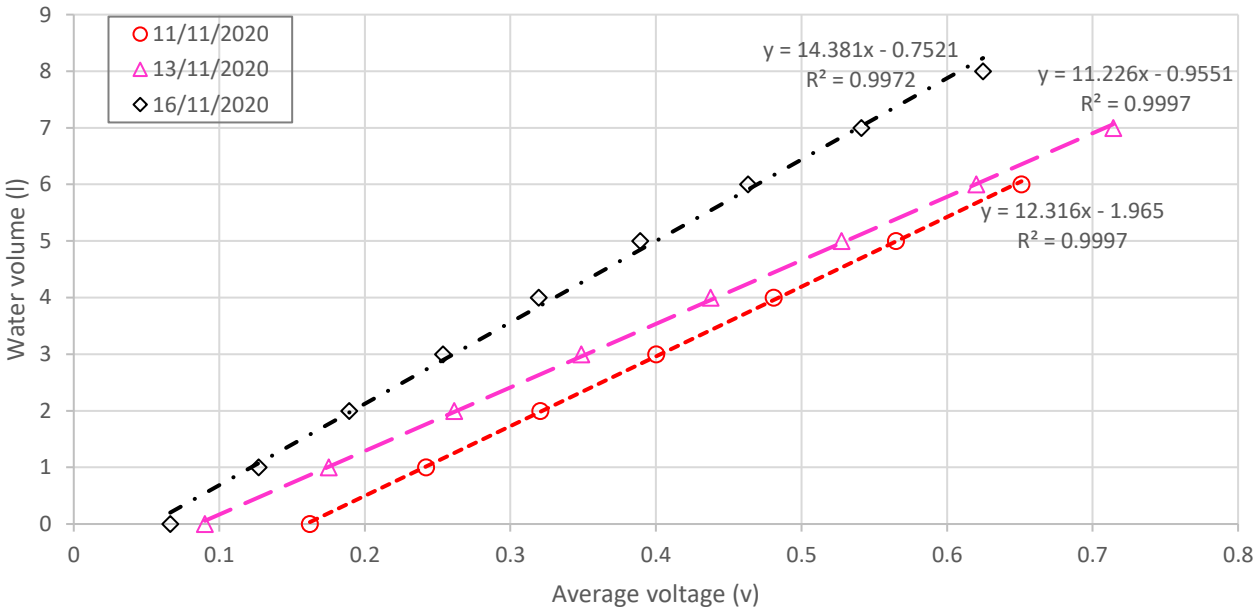


**Figure 12:** Depth gauge average voltage v. Water volume

## Wind

An anemometer was temporarily installed on top of the vertical wall so that the wind generator's output could be calibrated. As the anemometer's units were miles per hour (mph), five prototype target wind speeds of between 30 and 70 mph were selected from the Beaufort Scale (McDonald, 2019). Those wind speeds were then scaled down for the physical modelling tests using the Froude scaling rule by multiplying them by $21^{0.5}$ (Hughes, 1993), then converting them to m/s (see Table 1 below).

**Table 1**: Wind data for the physical modelling tests utilising the Froude scaling rule and then converted to m/s

| Wind case | Beaufort Scale (Force) | Beaufort description | Target full scale wind speed (mph) | Scaled down wind speed (mph) | Scaled down wind speed (m/s) | Wind generator power (%) |
|---|---|---|---|---|---|---|
| 1 | 6 | Strong breeze | 30 | 6.5 | 3 | 14.39 |
| 2 | 8 | Gale | 40 | 8.7 | 4 | 19.18 |
| 3 | 9 | Strong gale | 50 | 10.9 | 5 | 23.97 |
| 4 | 10 | Storm | 60 | 13.1 | 6 | 28.77 |
| 5 | 11 | Violent storm | 70 | 15.3 | 7 | 33.56 |

The wind generator's output was used to produce wind speed steps of 1 mph between 5 and 20 mph and, for each step, the % power on the generator was recorded. As the wind speed did not remain constant, accuracy was estimated to be ± 2 mph above 12 mph and ± 1 mph between 1 and 12 mph. This process was then repeated twice more, and the average power readings plotted against the wind speed, as seen in Figure 13 below. The gradient of the best fit line determined that the % power on the generator was 2.1973 times the scaled down wind speed. This value was then used to set the % power required for each wind case (see Table 1 above).

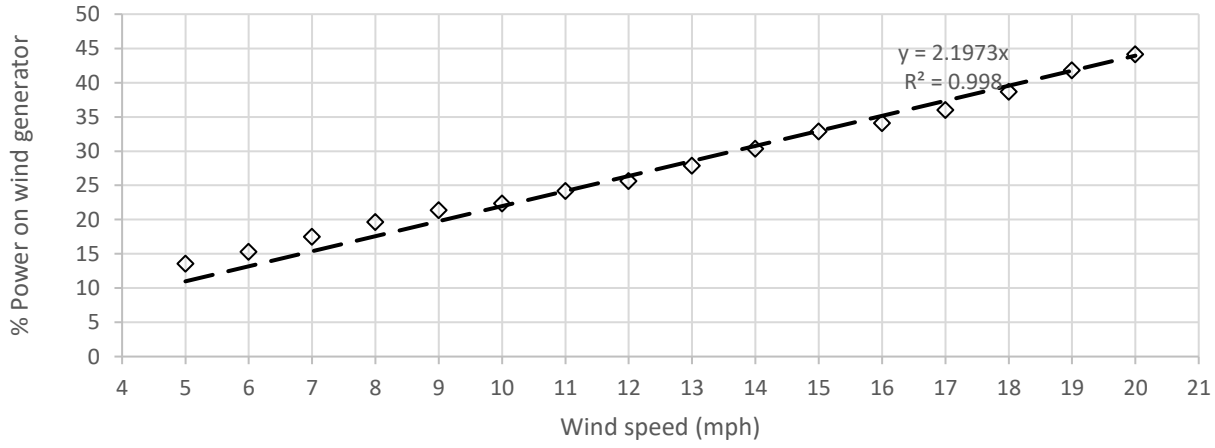


**Figure 13:** Scaled down wind speed v. % Power on wind generator

### Incident target wave conditions

Thirteen regular waves and seven irregular wave series were selected to provide types and magnitudes of overtopping that would show the influence of different applied wind speeds. Their (peak) frequencies were scaled down according to Strouhal similitude, which also satisfies Froude's scaling rule (Chakrabarti, 1998), by multiplying them by $21^{0.5}$. Table 2 below provides a summary of the regular wave incident target conditions and Table 3 below provides the equivalent irregular wave data. Each regular wave cycle had an amplitude of 0.045 m. Each of the irregular wave series had a JONSWAP spectrum.

**Table 2:** Regular wave incident target conditions

| Frequency (Hz) | Period (s) | Run Time (s) | Wave-length (m) |
|---|---|---|---|
| 0.40 | 2.500 | 25.000 | 6.256 |
| 0.45 | 2.222 | 22.219 | 5.427 |
| 0.50 | 2.000 | 20.000 | 4.754 |
| 0.55 | 1.818 | 18.182 | 4.194 |
| 0.60 | 1.667 | 16.667 | 3.713 |
| 0.65 | 1.538 | 15.385 | 3.304 |
| 0.70 | 1.429 | 14.286 | 2.950 |
| 0.75 | 1.333 | 13.333 | 2.645 |
| 0.80 | 1.250 | 12.500 | 2.370 |
| 0.85 | 1.176 | 11.765 | 2.128 |
| 0.90 | 1.111 | 11.111 | 1.930 |
| 0.95 | 1.053 | 10.531 | 1.747 |
| 1.00 | 1.000 | 10.000 | 1.588 |

**Table 3:** Irregular wave incident target conditions

| Peak frequency ($F_p$) (Hz) | Peak period ($T_p$) (s) | Physical model spectral period $T_{m-1,0}$ (s) [3] | Significant wave height ($H_{m0}$) (m) |
|---|---|---|---|
| 0.4000 | 2.4784 | 2.253 | 0.0699 |
| 0.5500 | 1.8024 | 1.639 | 0.0698 |
| 0.5634 | 1.7597 | 1.600 | 0.0698 |
| 0.6250 | 1.5862 | 1.442 | 0.0697 |
| 0.6993 | 1.4177 | 1.289 | 0.0695 |
| 0.8503 | 1.1659 | 1.060 | 0.0690 |
| 1.0000 | 0.9914 | 0.901 | 0.0682 |

[3] $T_{m-1,0} = T_p/1.1$ (Van der Meer et al., 2018)

### Selected tests

The initial intention was to use 30 wave cycles for each regular test and that each irregular wave series would run for 10 minutes. However, early testing showed that overtopping outside the equipment's range was produced for some frequencies at the stronger wind speeds. Therefore, regular wave runs were shortened to ten wave cycles, which kept them within test length limits suggested by the International Towing Tank Conference (ITTC, 2017). Irregular wave runs were shortened to three minutes. This length fell outside ITTC guidance that tests should be run at full-scale for at least one hour to allow stationary wave conditions to develop, equivalent to 13 minutes at a scale of 1:21 (ITTC, 2017). However, guidance was taken from Reis et al. (2018) that it is possible to obtain more information about overtopping from several short-duration tests than one lengthy one.

Regular waves were run with no wind and with each of the five wind cases (see Table 1 above). Unfortunately, it was not possible to run the irregular waves under either the Force 10 (WC4) or Force 11 (WC5) wind conditions because these produced overtopping that exceeded the equipment's range.

Recording continued for three minutes after the paddle had stopped producing waves so that any residual overtopping could drain into the collection container. The test was then stopped, and at that point, the wind generator was turned off. The tank was allowed to settle for approximately three minutes for regular waves and five minutes for irregular waves before the next test was run. A data file was saved for each test, and numerous videos were taken to capture the physical nature of the overtopping.

The following further investigations were carried out to check the accuracy of the collected data:

- to assess repeatability (ITTC, 2017), one of the wave runs was repeated for each of the wind cases;
- to check whether there was any reflection build up in the flume for the regular waves (ITTC, 2017), 30 wave cycles were run for each frequency (without wind); and
- to test whether shortening the run time to three minutes affected the development of the irregular wave spectra and resulting overtopping rates, all the irregular wave series were run without wind for 5 minutes, and two of them were run for 7.5 and 10 minutes.

## Overtopping predictions

### EurOtop formulae

Both the prediction and design and assessment versions of the EurOtop's formulae for vertical sea walls (Van der Meer et al., 2018) were applied to each of the irregular wave series to predict the mean value of q that would occur without the addition of wind. The specific formulae were selected based on the setup for the physical modelling tests. There was an influencing foreshore, no significant mound in front of

the structure's toe, a likelihood of impulsive overtopping conditions and a relative freeboard that exceeded 1.35.

Table 4 contains the calculated (scaled down) values for the mean value of q, converted to l/s per m. These values are compared to the test data.

**Table 4:** Predicted q based on the EurOtop formulae

| | q (l/s per m) | |
|---|---|---|
| Peak frequency (Hz) | Prediction formula | Design and assessment approach |
| 0.400 | 0.022 | 0.032 |
| 0.550 | 0.016 | 0.023 |
| 0.563 | 0.016 | 0.022 |
| 0.625 | 0.014 | 0.020 |
| 0.699 | 0.012 | 0.018 |
| 0.850 | 0.010 | 0.014 |
| 1.000 | 0.008 | 0.011 |

## Bayonet GPE online tool

The Bayonet GPE ANN tool (H R Wallingford, 2019) was used to predict overtopping for each of the irregular wave series. The tool produced an instantaneous prediction for the overtopping rate, coupled with a 95% confidence interval range. Each set of results was specified as "amber", defined in terms of the Mahalanobis distance from the input data to the nearest training data point as "marginally significant but acceptable". To see if "green" quality outputs could be obtained, the process was repeated with the parameters scaled up to prototype, but this made no difference.

Table 5 contains the results from the ANN, which are compared to the recorded test data.

**Table 5**: Predicted overtopping and confidence interval ranges from Bayonet GPE online tool

| **Peak frequency (Hz)** | **Predicted overtopping rate (l/s per m)** | **95% confidence interval range (l/s per m)** | |
|---|---|---|---|
| | | Lower limit | Upper limit |
| 0.400 | 0.0108 | 0.0000228 | 5.15 |
| 0.550 | 0.0108 | 0.0000227 | 5.12 |
| 0.563 | 0.0108 | 0.0000227 | 5.12 |
| 0.625 | 0.0108 | 0.0000226 | 5.11 |
| 0.699 | 0.0107 | 0.0000226 | 5.09 |
| 0.850 | 0.0106 | 0.0000223 | 5.04 |
| 1.000 | 0.0104 | 0.0000222 | 4.96 |

## Results and Discussion

### Regular waves – main results

No wind case

The “no wind” test series demonstrated the effect that wave frequency had on overtopping. Figure 14 shows a plot of frequency against q. Figure 15 below provides stills from videos taken during testing, for wave frequencies of 0.40, 0.60, 0.70 and 1.00 Hz.

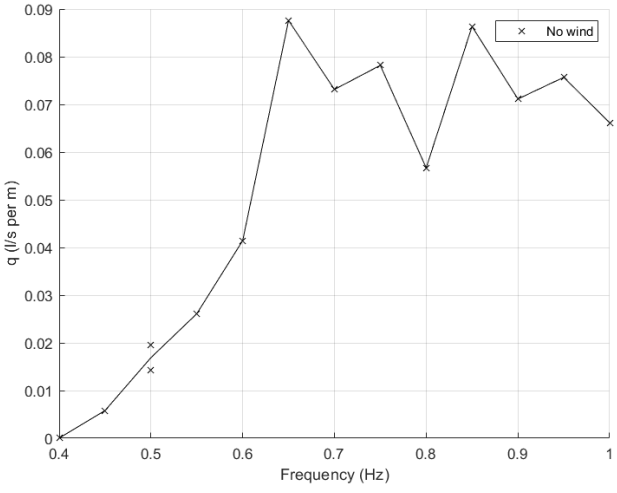

**Figure 14**: Frequency v q for no wind case (regular waves). NB: For the repeated test at 0.5 Hz, both results have been plotted, but the plot line runs through the average of those points.

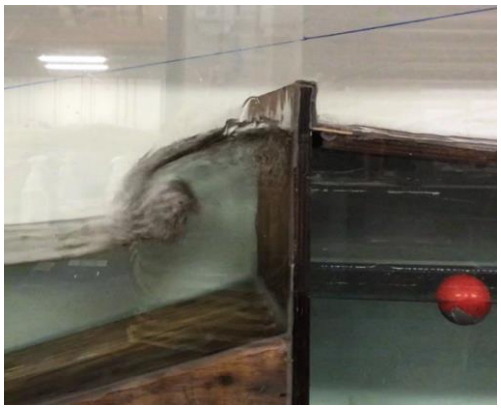

(a) 0.40 Hz – wave reflected by wall – no overtopping

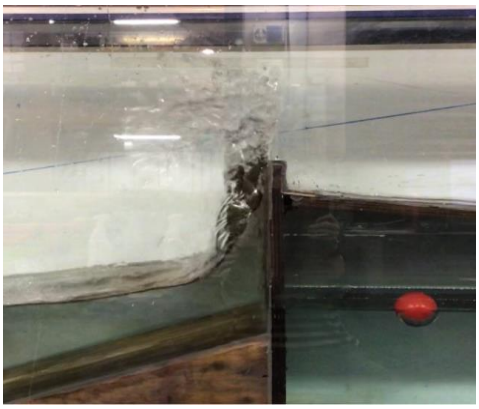

(b) 0.60 Hz – transition between green and impulsive overtopping

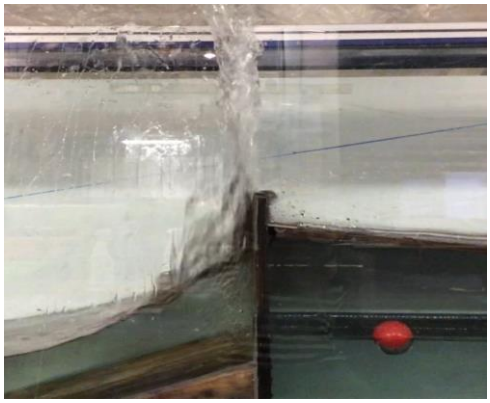

(c) 0.70 Hz – impulsive overtopping

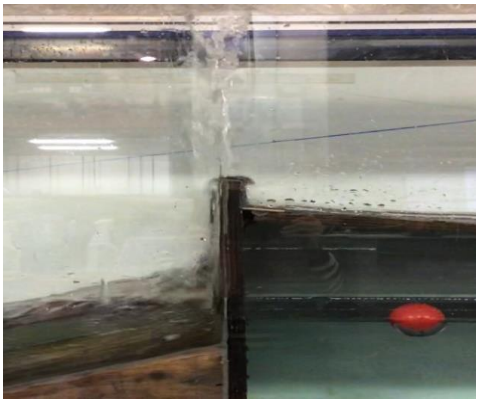

(d) 1.00 Hz – impulsive overtopping with a thinner plume of water

**Figure 15:** Video stills of regular wave overtopping (no wind)

Waves with a frequency of 0.40 Hz produced no overtopping. Whilst the waves ran up the wall, they did not reach its crest, and were reflected by the wall, as can be seen in Figure 15 (a) above. As the wave frequency increased, the run-up exceeded the wall's crest as green overtopping. By 0.60 Hz, the nature of the wave's interaction with the wall started to change. As shown in Figure 15 (b) above, the wave crest exceeded the wall's crest, splashing up into the air and producing a higher q than occurred for the lower frequency waves. At 0.65 Hz, q peaked (see Figure 14 above). At this frequency, the waves started to break on the slope a short distance before the wall, causing water to run up the wall and be thrown a

considerable distance into the air as impulsive overtopping. Figure 15 (c) above shows the impulsive overtopping produced by the 0.70 Hz wave. By 0.85 Hz, the nature of the waves' interaction with the wall again started to change, causing q to peak a second time (see Figure 14 above). The incident and reflected waves interacted in an irregular motion. This caused some waves to break further back from the wall, and those interacting with the wall either broke close to the wall or against the wall itself. The irregularity of the motion became more pronounced as the frequency increased to 1.00 Hz. Water was still thrown a considerable distance into the air but, as Figure 15 (d) above shows, the plume was much thinner than the impulsive jets produced by the 0.70 Hz frequency waves and, as a result, q reduced.

The effect of wind

Figure 16 below shows that the application of wind made a significant difference to q for all regular wave frequencies. For all frequencies, q for WC1 exceeded that for the no wind case, and q for WC5 exceeded that for WC1. However, the results for WC2 to WC4 showed much less predictability, particularly at the higher frequencies. There were several instances where q at a lower wind speed exceeded rates seen during tests with stronger winds, for example at 0.85 Hz for WC2.

The interaction between the waves and the wall changed as the wave frequencies changed. Whilst q peaked at different frequencies under different applied wind

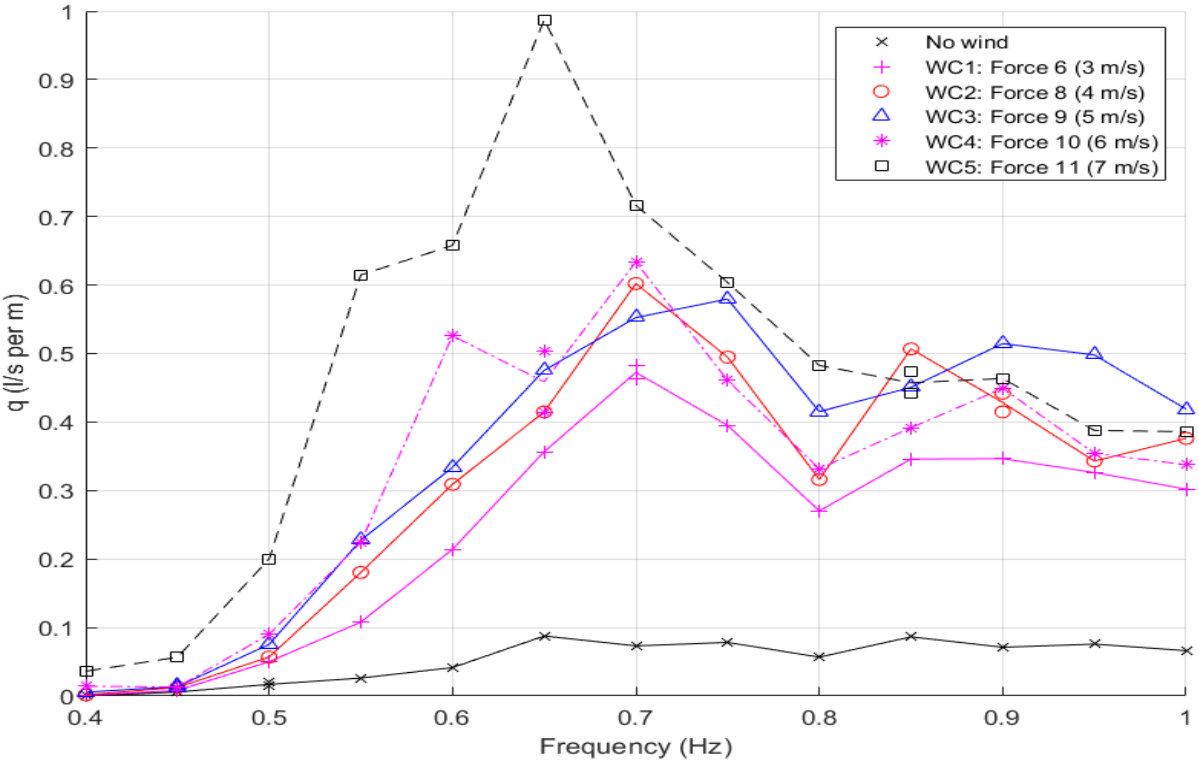


conditions, all the peaks occurred between 0.65 Hz and 0.75 Hz (see Figure 16 below). As described for the no wind case (see above), between these frequencies the interaction with the wall maximised possible overtopping.

**Figure 16**: Frequency v. q for all wind cases (regular waves). NB: For tests that were repeated, e.g. 0.9 Hz at WC2, both results have been plotted, but the plot line runs through the average of those points

The following paragraphs consider how the interaction between the mode of overtopping and the differing wind speeds affected q.

Wind had little effect on the waves with frequencies of 0.40 and 0.45 Hz (see Figure 17). This was because the wave crests only just reached the top of the wall and, therefore, there was only a small area of water to interact with the wind.

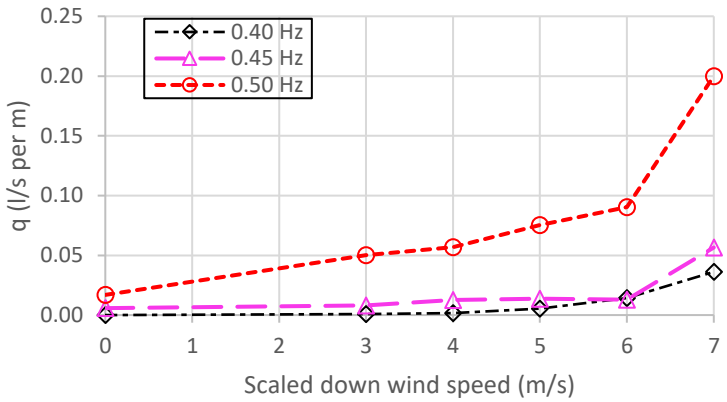


Figure 17: Applied wind speed v. q – 0.40 Hz to 0.50 Hz

(regular waves)

By comparison, a considerable increase in q was seen for the 0.50 Hz waves. Figure 18 below shows stills from videos taken during testing under the no wind and Force 10 (WC4) conditions. As the wave reached the wall's crest, rather than being reflected by the wall, the wind acted upon its upper section, thereby forcing the water over the wall. This effect became more pronounced under WC5 (Force 11).

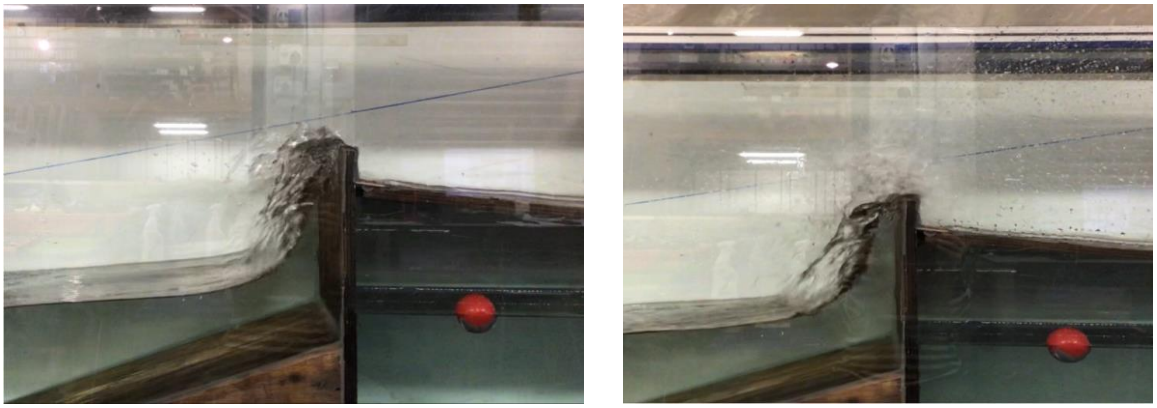

(a) No wind (b) Force 10 (WC4) conditions

Figure 18: Video stills of overtopping produced by 0.50 Hz regular wave

Between wave frequencies of 0.55 and 0.65 Hz, overtopping trends were mostly as expected, increasing with both frequency and applied wind strength (see Figure 19). There was a sharp peak in q under WC5 at 0.65 Hz (see Figure 23 above).

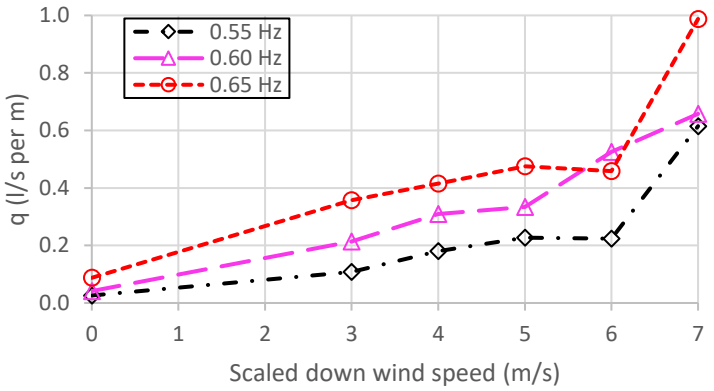


**Figure 19:** Applied wind speed v. q – 0.55 Hz to 0.65 Hz (regular waves)

For the 0.75 Hz wave, q was higher for both WC2 and WC3 than WC4, with WC3 producing almost the same overtopping as WC5 (see Figure 20). Figure 21 (a) and (b) below show video stills from tests at this frequency, under the Force 8 (WC2) and Force 11 (WC5) wind conditions.

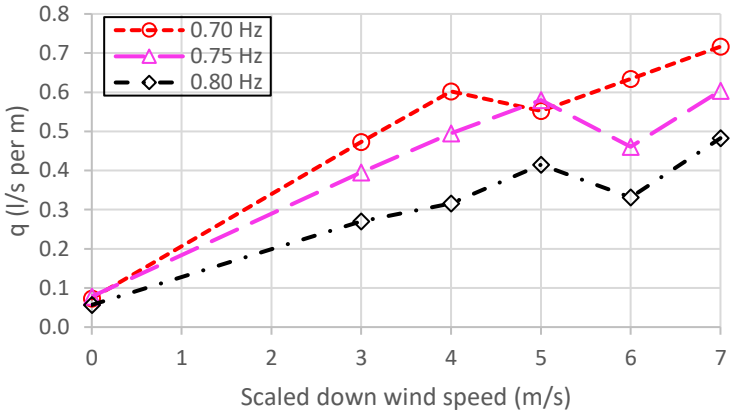


**Figure 20:** Applied wind speed v. q – 0.70 Hz to 0.80 Hz (regular waves)

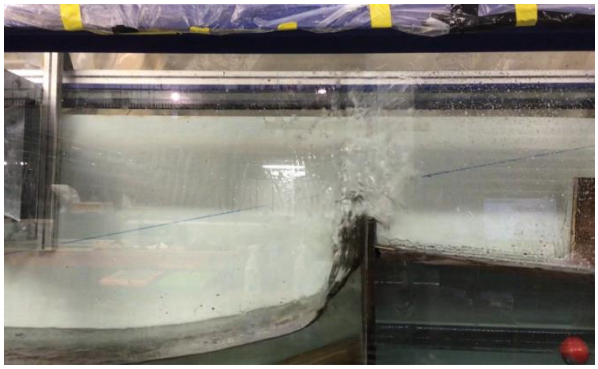

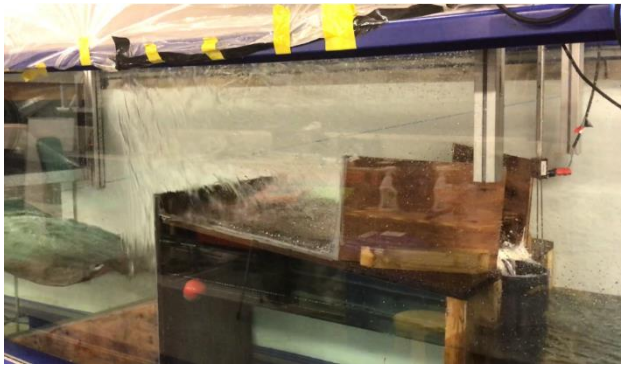

(a) Force 8 (WC2) conditions (b) Force 11 (WC5) conditions

Figure 21: Video stills of overtopping produced by 0.75 Hz regular wave

The influence of the Force 8 wind was enough to push the body of water produced by the impulsive overtopping past the wall's crest so that it landed on the run-off section and was captured in the overtopping container. By comparison, the Force 11 wind (WC5)'s influence was so significant that it broke up the body of impulsive overtopping, thereby sending some of the water beyond the overtopping container and causing some of it to be so aerated that it could not be captured. This inability to capture all the water passing over the wall's crest is accepted as an experimental limitation, meaning that q may not have been representative of the true situation at this frequency and wind speed.

Figure 22 shows that, for the high frequency waves of 0.85 Hz and above, q gradually levelled off as the wind increased and, in general, the highest values of q were produced by the Force 9 wind (WC3). The mid-range wind speeds were strong enough to push all the thin body of impulsive overtopping past the wall's crest, without causing it to break up (see Figure 15 (d) above).

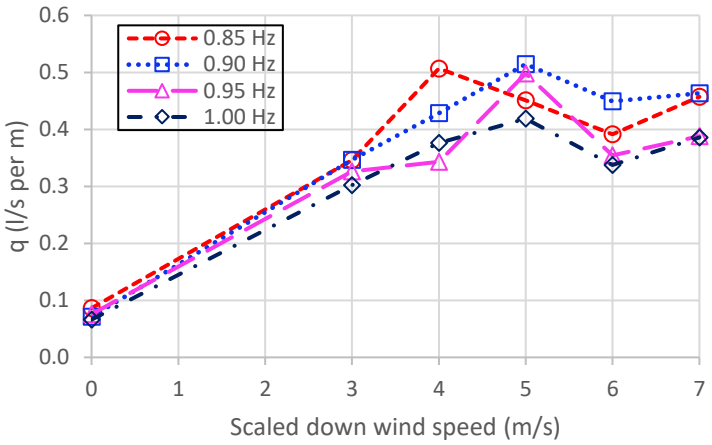


Figure 22: Applied wind speed v. q – 0.85 Hz to 1.00 Hz

(regular waves)

Therefore, as the wind increased further there was no more water available to overtop. With the higher wind speeds, the water became more aerated, so less of it travelled past the wall's crest into the overtopping container.

## Irregular waves – main results

Figure 23 shows a plot of peak frequency against q for each wind case.

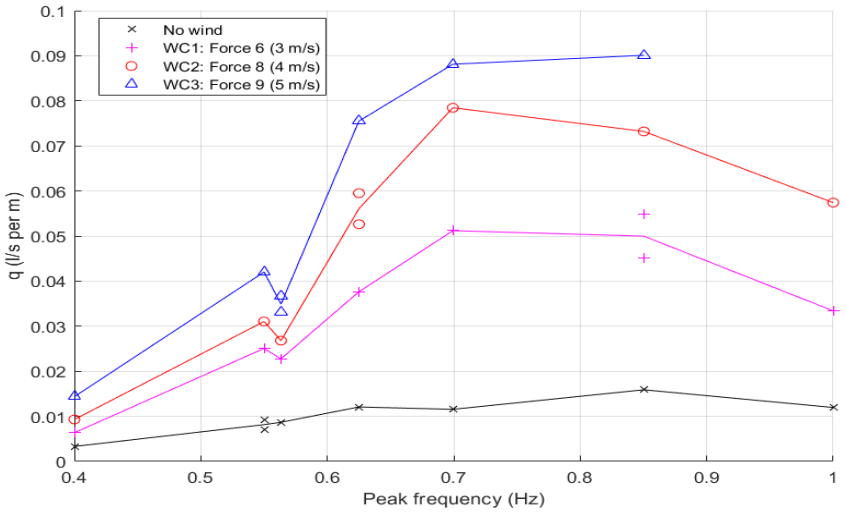


**Figure 23:** Peak frequency v. q for all wind cases (irregular waves). NB: For tests that were repeated, e.g. 0.6250 Hz at WC2, both results have been plotted, but the plot line runs through the average of those points.

### No wind case

Overtopping produced by the irregular waves was approximately one order of magnitude less than that produced by the regular waves of equivalent frequencies. This was because an irregular wave series produces waves with a spectrum of frequencies, specified by that spectrum's peak. This means that, unlike the regular waves, each wave propagating towards the wall was not the same size and did not produce the same overtopping. Despite these differences, videos of the tests showed that the transition between the different modes of overtopping occurred at around the same (peak) frequencies as described above for the regular waves. Also, q peaked twice (at 0.625/0.65 Hz and 0.850 Hz) for both types of waves.

### The effect of wind

Wind had a similar effect on the overtopping produced by the irregular waves as for the regular waves. Between the no wind case and the Force 9 conditions (WC3), regular wave overtopping increased by up to 770%[4] and irregular wave overtopping increased by up to 662%. What differed is that, for every irregular wave frequency, q increased with each increase in wind speed (see Figure 23 above).

[4] This statistic excludes the 0.4 Hz wave – as no overtopping occurred with no wind, the percentage calculation is not possible

Videos taken during the tests with applied wind show that, whilst not every wave propagating towards the wall overtopped, when overtopping occurred the wind/wave interaction was the same as for the regular tests (see above).

Figure 24 below show plots of the applied wind speed against q for each irregular wave series. There were some anomalies in these results, which cannot be explained. q for the wave series with a peak frequency of 0.550 Hz exceeded that for the 0.563 Hz wave series for all wind cases (see Figure 24 (a) below). Also, there was a distinct dip in q at the peak frequency of 0.563 Hz for all applied wind cases, which was not seen in the no wind case (see Figure 23 above). As no test was carried out for a regular wave at this frequency, it is not known whether similar results would have occurred.

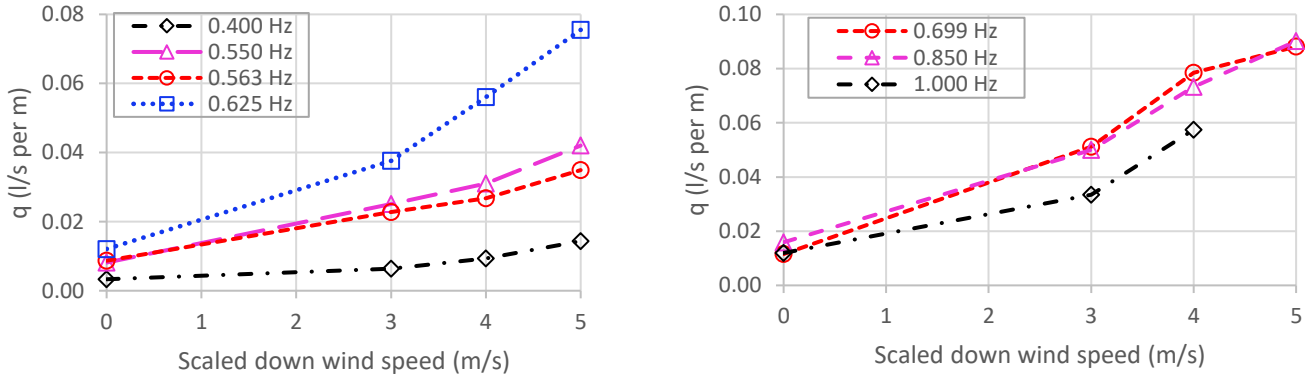


(a) 0.400 - 0.625 Hz

(b) 0.699 - 1.000 Hz [5]

**Figure 24**: Applied wind speed v. q (irregular waves)

As irregular waves with a peak frequency of 0.80 Hz were not tested, it is not known whether a similar dip in q would have been produced as was seen for the regular waves at this frequency, under all wind conditions (see Figure 16 above). It is also not known whether q would have levelled off for the irregular waves at the higher peak frequencies under the higher wind speeds, as occurred with the regular waves (see above).

### Regular waves – reflection coefficient check

A Matlab script was used to calculate the reflection coefficient ($K_r$) based on data recorded by the three wave gauges nearest to the vertical wall, on the paddle side of the structure (marked WG2 to WG4 in Figure 6 above). The values produced by the script will not be entirely accurate because it was designed to assess reflection from a vertical surface, whereas the steep slope in the flume would have affected wave propagation. Also, due to the short duration of each test, it was only possible to analyse data from five or six wave cycles.

[5] q for 1.000 Hz at WC3 could not be included because of a corrupt data file

For each dataset, the following steps were taken to determine an appropriate section of the wave data to be analysed:

- the wave number (k) was calculated using an iterative process for the equation shown in Figure 25 below, with an initial value of k based on the deep water approximation of $\omega^2/g$;
- the phase speed (c) was calculated (see Figure 25 below);
- the front trim time was calculated as the time taken for waves to travel from the paddle to the vertical wall and back to the third wave gauge (furthest from the wall) plus five additional wave periods – this was so that data would be measured once reflection had begun; and
- the end trim time was calculated as the front trim time plus five wave periods – this was so that measurement of the data would stop before the waves stopped.

$c = \omega/k$

$\omega = 2\pi f$

$$k = \frac{\omega^2}{g \tanh(kh)}$$

c = wave celerity (m/s)

ω = angular frequency ($s^{-1}$)

f = frequency (Hz)

k = wave number ($m^{-1}$)

g = acceleration due to gravity = 9.81 $m/s^2$

h = water depth (m)

Figure 25: Linear wave equations

Figure 26 below shows an example of the raw results produced for each wave frequency under each wind condition. The section between the two red lines on the top graph was the data that was analysed. The second graph provides a comparison between the measured wave data and the equivalent expected wave pattern as calculated by the Matlab script. As these two lines are very similar, confidence can be gained about the likely accuracy of the measurements.

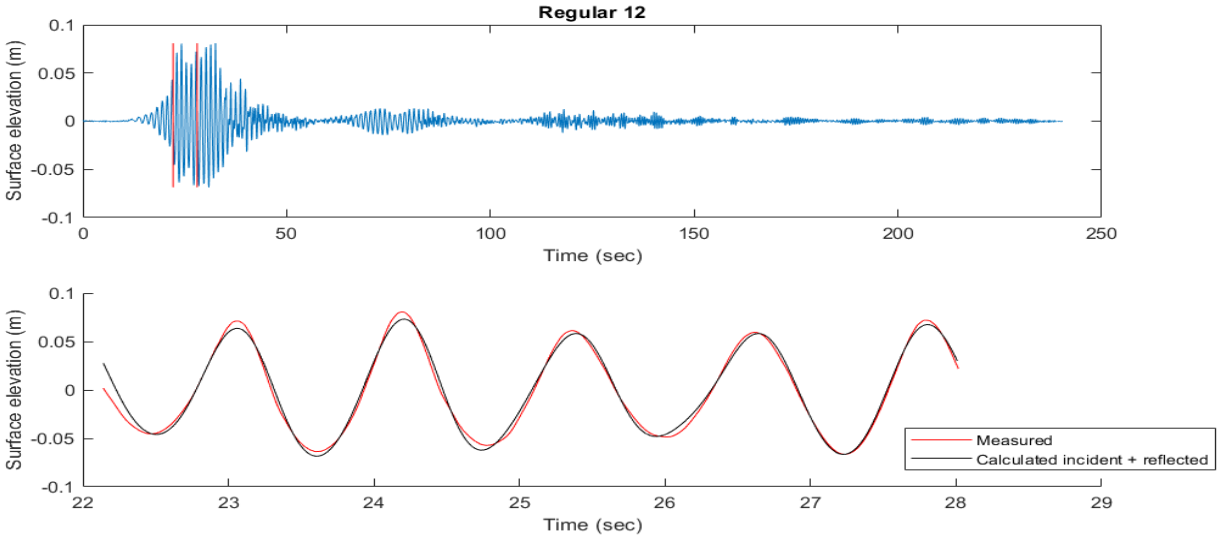

Figure 26: Sample reflection coefficient calculation – raw results – 0.85 Hz (no wind)

Figure 27 provides plots of frequency against $K_r$ for each of the wind conditions. (a) shows the results from the trim time as explained above. (b) and (c) below provide the same data, with the trim time altered by ± 2 seconds.

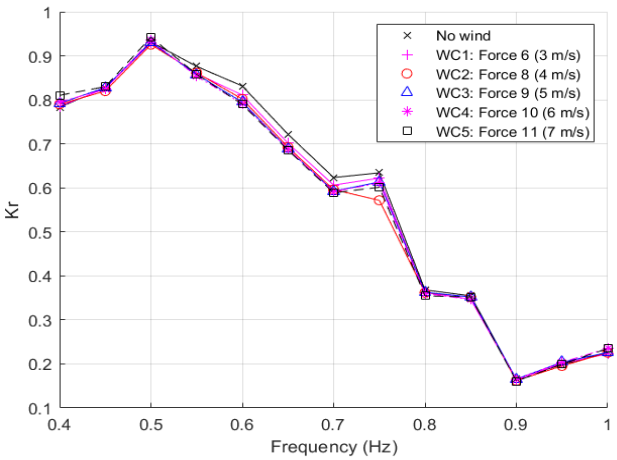


Figure 27: (a) Frequency v. Kr (regular waves) – original trim time

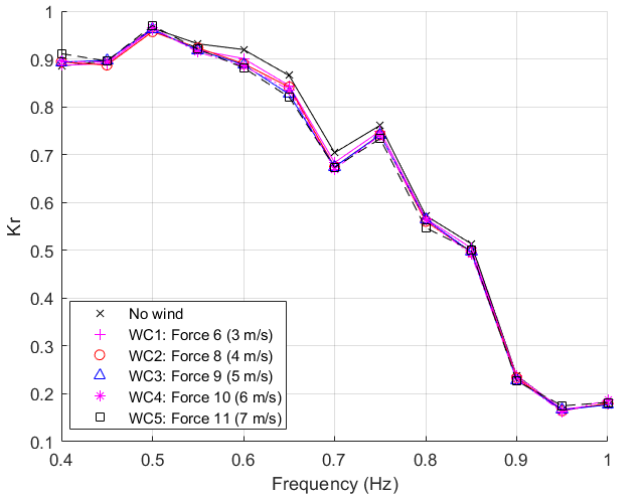


(b) trim time + 2 secs

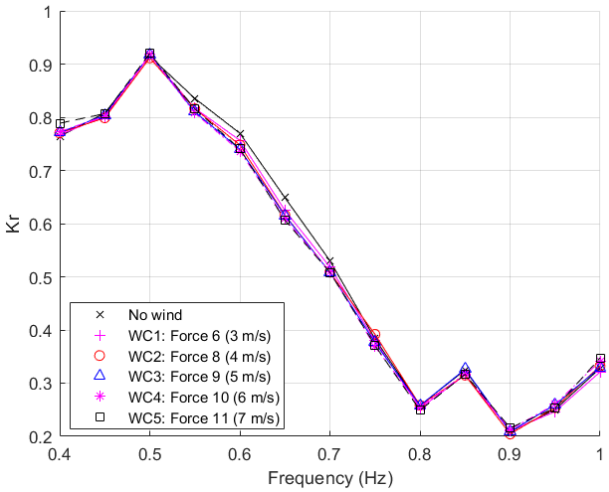


(c) trim time – 2 secs

Figure 27: (b) & (c) – Frequency v. Kr – trim time ± 2 seconds

Whilst the amount of reflected wave is not constant in the above figures, the trends are. Each of the three plots show that the wave frequency had a large bearing on the value of $K_r$. By comparison, the reflection of the incident waves hardly changed as the applied wind speed increased. The small reductions that were produced are likely to have been caused by there being less reflected energy due to overtopping.

As seen in Figure 23 above, the involvement of wind significantly affected q produced by the impulsive waves, of frequencies between 0.60 and 0.75 Hz.

However, Figure 27 above shows that the wind's impact on the reflection of these waves was minimal.

**Impact of run time**

Tests without wind, using both regular and irregular waves, were conducted to assess the impact of run time on the build-up of reflected wave energy within the flume.

Figure 28 shows a plot of frequency against q for each of the regular waves, using 10 and 30 wave cycles. Had there been no wave energy reflection, the plot lines would have been identical. However, there was a significant difference in q at various frequencies, with the most notable example occurring at 0.40 Hz. At this frequency, the test with 10 wave cycles produced no overtopping whereas 30 wave cycles produced q of 0.168 l/s per m.

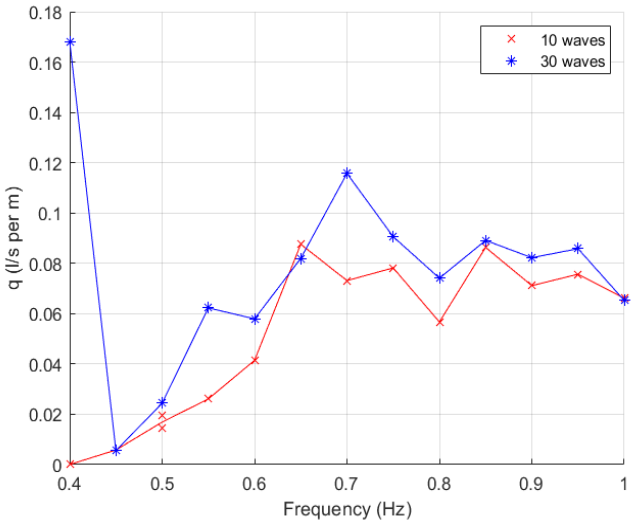


Figure 28: Run time check – regular waves

Figure 29 shows the results for the irregular wave tests. One was carried out for all peak wave frequencies, with run times of 3 and 5 minutes (Figure 29 (a)). The other used spectra with peak frequencies of 0.400 Hz and 1.000 Hz for 3, 5, 7.5 and 10 minutes (Figure 29 (b)). Had there been no wave energy reflection, the plot lines in Figure 29 (a) would have been identical, and the plot lines in Figure 29 (b) would each have been horizontal. However,

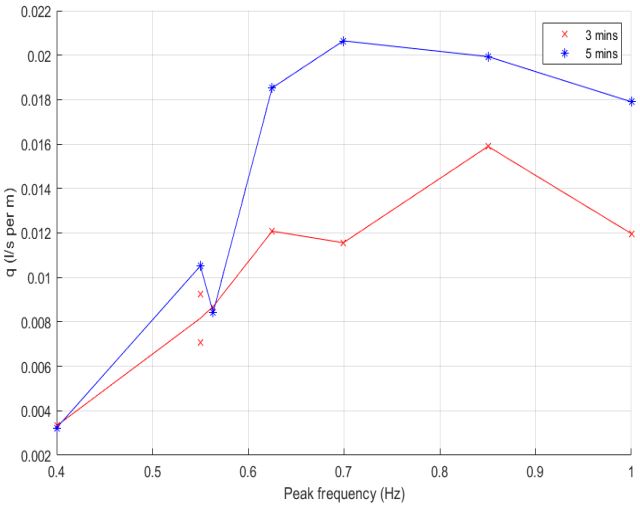


(a) all wave series - run times of 3 & 5 mins

considerable differences were again seen between the q rates.

These results suggest that it was appropriate to limit the test lengths for both the regular and irregular waves so that the data was not skewed by the presence of reflected energy.

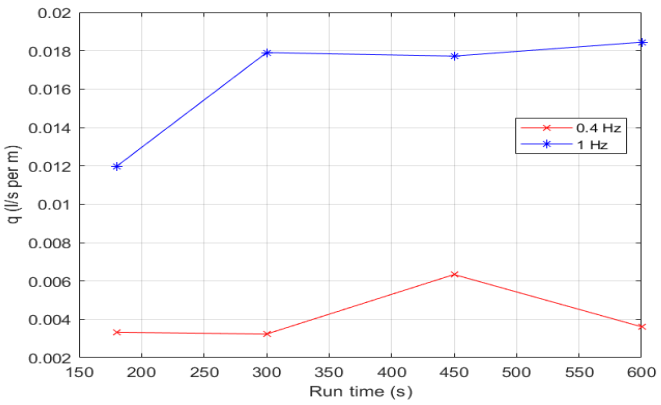


(b) peak frequencies of 0.400 & 1.000 Hz – run times of 3 to 10 mins

Figure 29: Run time checks – irregular waves

## Further discussions

The results of the physical modelling tests for the irregular waves ("the test results") were scaled up to prototype to allow comparison with findings from the research papers described above, and the outputs from the EurOtop formulae and the Bayonet GPE ANN (see above). Frequency was multiplied by $21^{-0.5}$ (Chakrabarti, 1998) and q was multiplied by $21^{1.5}$ (Hughes, 1993).

Data contained within the following sections all given at prototype unless otherwise stated.

### Test results v. research papers

The test results support Ward et al. (1994)'s conclusions that overtopping estimates not including wind effects would be too low, and that applied wind produced large increases in overtopping. Table 6 shows that q increased by between 4 and 7.6 times between the no wind and the Force 9 (WC3) conditions.

The test results do not support Ward et al. (1996)'s findings that the increase in q due to wind was large when the discharge rate was low, but that the wind's effect decreased as q increased (a conclusion that has since been supported by Pullen et al., 2009). The test results showed that the wind's effect was more strongly related to the wave's peak frequency (see Figure 23 above). Whilst the flume size for Ward et al. (1996)'s experiment (36 m long, 0.6 m wide and 0.9 m deep) was similar to that used in the physical modelling tests, there were fundamental differences in their setup, which may explain the differing results. They principally concentrated on revetment slopes (1:1.5, 1:3 and 1:5), the wind was applied 24 m back from the revetment and they varied wave height whilst retaining a constant wave frequency, whereas the opposite was true for the tests upon which this paper is based.

The wind adjustment factor ($f_{wind}$) suggested by de Rouck et al. (2005) and Pullen et al. (2009) (see Figure 3 above) was applied to the no wind test results and the adjusted values compared with the recorded data under the Force 9 (WC3) conditions. Table 7 below shows that the test results exceeded the adjusted values by a factor of between 3 and 7, with the most significant disparity occurring at the peak frequency of 0.153 Hz, when impulsive overtopping was at its maximum.

**Table 6:** Overtopping rates for irregular waves under no wind and Force 9 (WC3) conditions, scaled to prototype

| **Peak frequency (Hz)** | **q @ no wind (l/s per m)** | **q @ Force 9 (l/s per m)** | **Ratio q @ Force 9: q @ no wind** |
|---|---|---|---|
| 0.087 | 0.32 | 1.38 | 4.3 |
| 0.120 | 0.79 | 4.04 | 5.1 |
| 0.123 | 0.84 | 3.36 | 4.0 |
| 0.136 | 1.16 | 7.27 | 6.3 |
| 0.153 | 1.11 | 8.48 | 7.6 |
| 0.186 | 1.53 | 8.67 | 5.7 |

**Table 7:** Comparison between test results and wind adjusted values, scaled to prototype, per de Rouck et al. (2005) and Pullen et al. (2009)

| Peak frequency (Hz) | Recorded data @ no wind ($m^3$/s per m) | $f_{wind}$ | $q_{wind}$ ($m^3$/s per m) | $q_{wind}$ (l/s per m) | Recorded data @ WC3 (l/s per m) | Ratio of recorded data @ WC3 : $q_{wind}$ |
|---|---|---|---|---|---|---|
| 0.087 | 3.20E-04 | 1.37 | 4.39E-04 | 0.44 | 1.38 | 3.15 |
| 0.120 | 7.85E-04 | 1.15 | 9.03E-04 | 0.90 | 4.04 | 4.48 |

| | | | | | | |
|---|---|---|---|---|---|---|
| 0.123 | 8.36E-04 | 1.14 | 9.53E-04 | 0.95 | 3.36 | 3.53 |
| 0.136 | 1.16E-03 | 1.09 | 1.27E-03 | 1.27 | 7.27 | 5.73 |
| 0.153 | 1.11E-03 | 1.10 | 1.22E-03 | 1.22 | 8.48 | 6.95 |
| 0.186 | 1.53E-03 | 1.06 | 1.62E-03 | 1.62 | 8.67 | 5.35 |

De Rouck et al. (2005) and Pullen et al. (2009) applied wind directly in front of the sea wall, which was the approach taken during the physical modelling tests upon which this paper is based. However, the design parameters for the tests differed considerably. De Rouck et al. and Pullen et al. used a scale of 1:40, with a flume that was 20 m long, 0.4 m wide and 0.7 m deep. There was a moveable impermeable beach with a small gradient of 1:50. They selected 8 combinations of wave period and wave height to reproduce conditions seen in the field during storms at Samphire Hoe. At the toe of the structure, wave heights varied between 1.44 and 2.49 m, wave periods were 5.59 to 7.29 seconds, the water depth range was 3.4 to 5.92 m, and the crest freeboard ranged from 5.59 to 8 m. By comparison, the physical modelling tests upon which this paper is based had a much steeper slope (1:3 gradient), a fixed water depth at the toe of 1.05 m, a fixed significant wave height of 1.47 m and a fixed crest freeboard of 5.25 m. It is suggested that the minimal depth at the toe of the structure may account for the larger variance in the test results than from the use of $f_{wind}$, which was derived for deeper water. The wave interaction with the wall may have been more impulsive than would have occurred in de Rouck et al. (2005) and Pullen et al. (2009)'s setup. As a result, larger volumes of water might have been thrown into the air, which increased q.

Pullen et al. (2009) commented that some observations of $f_{wind}$ may have shown it to be of the order of a magnitude or more, but that the maximum value of four was recommended by de Rouck et al. (2005). If the order of magnitude observations were to be preferred, then this would bring the test results in line with what might be expected. As stated above, q increased by up to 7.6 times between the no wind and the Force 9 (WC3) conditions (see Table 6 above).

The test results partly support Murakami et al. (2019)'s findings of a dependency between the wind velocity's influence and the wave period. This is interesting when considering the similarities between the setup of the two experiments. Murakami et al. used an exhaust fan to generate wind up to 8 m/s (believed to be at scale). At scale, the water depth in the tank was 0.66 m, and the water depth at the toe of the vertical structure was 0.05 m. The significant wave height was 0.07 m, and wave periods of between 1.2 and 2 seconds were used. However, the flume was only 15 m long, and the wind was applied at its end instead of just in front of the wall. The slope in front of the vertical structure was 1:10 (instead of 1:3), and the crest freeboard was smaller (0.07 m instead of 0.25 m). Converting Murakami et al. (2019)'s comments to relate to peak frequency instead of period, they stated that longer wave frequencies produced a larger difference between the no wind and wind applied overtopping than shorter wave frequencies. Whilst the dependency between

wind velocity and frequency was seen in the test results, the wind had a lesser effect at the higher peak frequencies of 0.186 Hz and above.

Only some of Iwagaki et al. (1966)'s findings fall within the range of the conducted tests. Also, their experiment was set up in a different way to the one on which this paper is based. They used an enclosed wind tunnel and applied the wind approximately 20 m back from the vertical wall. Further, they varied both the water depth at the toe of the structure and the crest freeboard. In relation to their finding that overtopping suddenly increased for incident waves that did not break in front of the sea wall when the wind reached a certain velocity, Iwagaki et al.'s results for $V/\sqrt{(gH_0)}$ of 6 to 7 with a wave steepness of 0.01 are comparable to the test results for the peak frequency of 0.087 Hz under the Force 9 conditions (WC3). Also, the results for $V/\sqrt{(gH_0)}$ of 3 to 5 with a wave steepness of 0.02 are equivalent to the test results with peak frequencies of between 0.120 and 0.136 Hz under the Force 6 and Force 8 conditions (WC1 and WC2). Whilst Iwagaki et al. do not define the rapid increase, Figure 24 (a) above shows an equivalent noticeable increase in q for the above range.

Iwagaki et al. (1966)'s statement about overtopping caused by waves that broke just in front of the sea wall (causing water to rise high above the wall) has been assumed to relate to the higher frequency waves within the physical modelling tests, of 0.186 Hz and above. Whilst it was not possible to test these waves at the higher wind speeds, it is reasonable to assume that they would have continued to behave in a similar way to the regular waves. Iwagaki et al. found that when $V/\sqrt{(gH_0)}$ was 5 to 7, the overtopping rate decreased. They suggested that the water drops might have been so fine that they could not be collected in the overtopping tanks. The results for the regular waves (see Figure 16 above) show that the effect of wind started to level off at these higher frequencies (which had scaled values of 0.85 Hz and above). Whilst Iwagaki et al.'s reasoning might be correct, it is also suggested that the higher wind speeds caused the water to become so aerated that less of it passed over the wall's crest.

As none of the analysed experiments had the same design parameters as the physical modelling tests, it is not surprising that the results varied. However, the trend was that the wind's influence during the physical modelling tests exceeded that found during some of the other studies, with the most significant disparity occurring when impulsive overtopping was at a maximum. This may have occurred because the physical modelling tests had very shallow water at the toe of the structure, which heightened impulsive interaction between the water and the wall, resulting in a greater volume of water being thrown into the air and, therefore, available to pass over the wall's crest.

Whilst the specific values within the results may not represent reality, it is submitted that the trends do. It is accepted that it is impossible to scale wind accurately within a physical modelling test. However, the general view from published studies is that wind will be under-scaled by Froude's law, compared to real-life conditions. If this is true, then the significant effects of wind on overtopping seen during the tests would be even more pronounced in real-life.

### No wind test results v. EurOtop and Bayonet GPE ANN predictions

Table 8 below compares the test results without the addition of wind with the mean values of q produced by the EurOtop manual's prediction formulae and the Bayonet GPE ANN's output.

**Table 8**: Comparison of measured and predicted q, scaled to prototype – irregular waves (no wind)

| Peak frequency (Hz) | q (l/s per m) | | | | | Ratio of physical modelling results : overtopping predictions | |
|---|---|---|---|---|---|---|---|
| | Physical modelling tests (without wind) | EurOtop over-topping predict-ion | Bayonet GPE | | | | |
| | | | Over-topping predict-ion | 95% confidence interval lower limit | 95% confidence interval upper limit | EurO-top, 1: | Bayo-net GPE, 1: |
| 0.087 | 0.32 | 2.15 | 1.04 | 0.002194 | 496 | 6.7 | 3.2 |
| 0.120 | 0.79 | 1.55 | 1.04 | 0.002185 | 493 | 2.0 | 1.3 |
| 0.123 | 0.84 | 1.51 | 1.04 | 0.002185 | 493 | 1.8 | 1.2 |
| 0.136 | 1.16 | 1.36 | 1.04 | 0.002175 | 492 | 1.2 | 0.9 |
| 0.153 | 1.11 | 1.20 | 1.03 | 0.002175 | 490 | 1.1 | 0.9 |
| 0.186 | 1.53 | 0.95 | 1.02 | 0.002146 | 485 | 0.6 | 0.7 |
| 0.218 | 1.15 | 0.77 | 1.00 | 0.002136 | 477 | 0.7 | 0.9 |

The test results broadly support Van der Meer et al. (2018)'s guidance that the EurOtop manual's predictions can only be taken to be within a factor of one to three of actual overtopping rates and that the largest deviations will occur when q is low. Table 8 above shows that the only wave series that fell outside this guidance was that with a peak frequency of 0.087 Hz, where the predicted mean value of q was 6.7 times higher than the test result.

The Bayonet GPE ANN overestimated overtopping for the 0.087 Hz peak frequency wave series by a factor of 3.2, and slightly underestimated q for the wave series with a peak frequency of 0.218 Hz by a factor of 0.9. However, what is most striking (and potentially alarming) about the output is that the 95% confidence interval was from effectively no overtopping to at least 475 l/s per m (see Table 8 above). This upper

limit is far beyond any acceptable limits for people or structures (Van der Meer et al., 2018), and the range is so broad that it would make it impossible to have confidence in selected design parameters.

### Test results v. EurOtop manual's guidance about the effect of wind

The test results have been compared with the mean values of q produced by the EurOtop manual's design and assessment formulae (Van der Meer et al., 2018) (see Figure 30 below). The design and assessment mean values were selected in preference to outputs from the prediction formulae because of the inclusion of a partial factor of safety to cover uncertainties. Also, the design and assessment formulae would be used when designing new structures. Further, the manual's stated accuracy level (Van der Meer et al., 2018) has been considered by including a comparison with tripled design and assessment values ("the tripled design values").

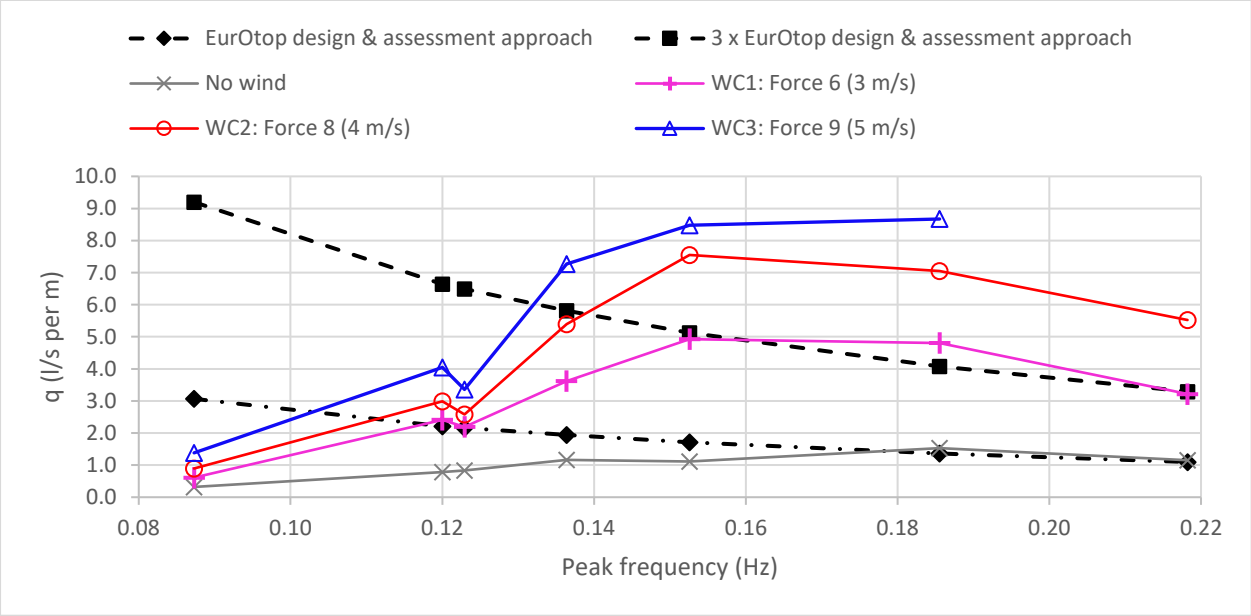


**Figure 30:** Comparison of irregular wave series test data and EurOtop design & assessment formulae predictions, scaled to prototype

Green overtopping

This section considers the test results for waves that produced green overtopping, with peak frequencies of up to 0.123 Hz.

The EurOtop manual states that green overtopping of less than one l/s per m can increase by up to four times under strong winds (Van der Meer et al., 2018). However, the test results suggest that this might be an underestimation. Under the Force 9 conditions, overtopping produced by the wave series with a peak frequency of 0.120 Hz increased by over five times (see Table 6 above). Had that wave series been subjected to higher wind speeds, this figure would inevitably have increased.

It is relevant to consider whether the higher than predicted overtopping rates could be covered by the tripled design values. Figure 30 above shows that q remained

well below those tripled values for WC1 to WC3. Had the irregular waves continued to produce q of one order of magnitude less than the regular waves (see above), it is likely that q under the Force 11 (WC5) conditions would still have been less than the tripled design values. Therefore, the test results suggest that the EurOtop design and assessment formulae (plus accuracy limits) adequately account for the wind's effect on low rates of green overtopping.

Impulsive overtopping

This section considers test results for waves that produced impulsive overtopping, with peak frequencies of 0.136 Hz and above.

The test results support the EurOtop manual (Van der Meer et al., 2018)'s statement that wind effects might increase as overtopping becomes more impulsive. However, they do not support the manual's suggestion that whilst wind might affect impulsive overtopping discharges of less than a few l/s per m, that effect is likely to be subsumed within the formulae's 90% confidence band.

The combination of impulsive overtopping and applied wind produced q that exceeded the tripled design values for all peak frequencies (see Figure 30 above). For the 0.153 Hz wave series, when impulsive overtopping was at a maximum, the threshold was passed under the Force 8 conditions and, under the Force 9 wind, q almost reached twice the tripled design value.

Had the irregular waves continued to produce q at approximately one order of magnitude less than the regular waves, the Force 11 (WC5) conditions might have produced a considerable increase in impulsive overtopping at peak frequencies of 0.136 and 0.153 Hz. This is likely because those peak frequency waves produced overtopping beyond the limits of the equipment at the start of the testing process, which resulted in the test length being reduced. Any such increase in q would have widened the disparity between the tripled design values and the test results.

Concerns about this disparity heighten when considering the industry-accepted issues surrounding the scaling of wind (see above). Accepting the recommendation that wind scaled according to Froude's law should be considerably increased to make it compatible with real-life conditions would mean that the values of q at prototype would be even greater.

## Wider design considerations

The outputs from the EurOtop manual's design and assessment formulae (Van der Meer et al., 2018) produced mean values for q based on a single set of structural and hydraulic parameters. However, when a vertical sea wall is designed, a range of those parameters will always be considered. Therefore, it is appropriate to review whether the increase in overtopping produced by wind could make any difference to those design decisions.

Vertical sea walls are often capped with solid concrete that can withstand heavy overtopping. Therefore, tolerable overtopping limits are frequently determined by land usage behind the structure (Van der Meer et al., 2018). The EurOtop manual suggests that for the prototype significant wave height of 1.5 m, q should not exceed

approximately 5 l/s per m for pedestrians with access behind the sea wall, and 40 – 50 l/s per m for vehicles (Van der Meer et al., 2018).

Whilst these values suggest that the demonstrated effect of wind on overtopping is unlikely to change design decisions made to accommodate vehicle usage, the same cannot be said for use by pedestrians. The no wind test results produced a range for q of between 0.3 and 1.5 l/s per m, which increased to between 1.3 and 8.7 l/s per m under the Force 9 (WC3) conditions (see Table 6 above). Waves producing impulsive overtopping exceeded the suggested limit for pedestrians of approximately 5 l/s per m, and it is expected that q would increase under stronger wind conditions.

## Conclusions and Recommendations

The physical modelling tests could not be completed as initially planned due to equipment limitations. However, the obtained results enabled detailed analysis to be completed about the direct impact of wind on q, the effect of reflected wave energy within the flume and the wind's effect on the waves that were reflected by the wall.

The results for the regular waves showed that overtopping was strongly related to the wave's frequency. Up to a prototype frequency of approximately 0.130 Hz, green overtopping occurred. After that impulsive overtopping was seen. However, from 0.186 Hz the nature of the waves' interaction with the wall started to change, resulting in a thinner plume of water being thrown into the air and a reduction in q. The nature of the overtopping produced by the irregular waves was similar to that produced by the regular waves. However, it was approximately one order of magnitude less because not every wave propagating towards the wall overtopped.

The wind had a significant effect on overtopping at all frequencies. Between the no wind case and the Force 11 conditions, the overtopping produced by the regular waves increased by up to 2254%; between the no wind case and the Force 9 conditions, the irregular wave overtopping increased by between 4 and 7.6 times. However, the wind's effect was most pronounced between prototype (peak) frequencies of 0.13 Hz and 0.17 Hz when the overtopping was at its most impulsive. The regular wave results showed that from a prototype frequency of approximately 0.186 Hz, the wind's effect started to level off. This was because the mid-range wind conditions were strong enough to push the thin body of water above the wall's crest past the crest without causing it to break up. As the wind increased, there was no extra water available to overtop, and as the higher wind speeds made the water more aerated less of it travelled past the wall's crest into the overtopping container.

Analysis of the regular wave data showed that, whilst the wave frequency had a significant bearing on the value of the reflection coefficient, the reflection of the incident waves hardly changed as the applied wind speed increased. Wind significantly affected q produced by the impulsive waves of prototype frequencies between 0.131 and 0.164 Hz, but its impact on the reflection of those waves was minimal.

The key questions posed at the start of this paper are answered below.

*Can the results obtained during the physical modelling tests be relied on given the issues surrounding the simultaneous scaling of wind and waves?*

As it is not possible to accurately scale wind and waves simultaneously, the test results have accuracy limitations, especially at the higher wind speeds. The wind applied during the tests tended to have more influence on q than occurred in other experiments. This increased influence may have been due to the shallow water depth at the toe of the wall, which caused overtopping that was more impulsive than would have occurred in deeper water. Some model effects were seen within the run time tests, and the irregular waves produced some unexplained anomalies. However, the repeated tests produced results within the same order of magnitude, and regular and irregular waves produced the same type of overtopping at the same (peak) frequencies. Therefore, whilst the specific values within the test results may not represent reality, it is suggested that it would be appropriate to rely on the trends within those results.

*Did the results from the physical modelling tests concur with the EurOtop manual (Van der Meer et al., 2018)'s limited guidance about the effect wind has on overtopping?*

The test results suggest that the EurOtop manual's design and assessment formulae (plus accuracy limits) adequately account for the wind's effect on low rates of green overtopping.

The test results support the manual (Van der Meer et al., 2018)'s statement that wind effects might increase as overtopping becomes more impulsive. However, they do not support the manual's suggestion that those effects on overtopping discharges of less than a few l/s per m are likely to be subsumed within the formulae's 90% confidence band. Measured q exceeded the tripled design values at relatively low wind speeds. It is anticipated that, with increased wind, q would also increase, thereby widening the disparity between the tripled design values and the test results.

*Does it matter that wind effects are not accounted for within the EurOtop formulae?*

This paper's findings suggest that design decisions that do not fully consider the wind's effect on overtopping might result in vertical sea walls that are too low to limit that overtopping to acceptable rates, when strong onshore winds influence it. This risk is particularly true if the area behind the sea wall is to be used by pedestrians. During the tests, the Force 9 wind conditions produced q that would have exceeded the suggested prototype limit for that usage.

These concerns are heightened if it is accepted that wind scaled according to Froude's law should be increased to make it compatible with real-life conditions. Also, as climate change causes more extreme weather conditions and rising water levels, the probability of sea walls being overtopped will increase, and the need to include the effects of wind on overtopping in design decisions will become increasingly important.

## Recommendations and future work

It is recommended that further tests are completed for the irregular waves with a different overtopping catchment system that can cope with both low and higher rates of q. Waves could then be tested under the higher wind speeds (Force 10 and 11) to assess whether overtopping starts to level off at the higher (peak) frequencies, as occurred with the regular waves. It would also provide an opportunity for the run time to be increased in line with ITTC guidance (ITTC, 2017). Further, it is recommended that the whole experiment be repeated at a larger scale to assess scale effects.

## Acknowledgements

The writer would like to thank Dr Martyn Hann for his guidance throughout the drafting process, and the laboratory technicians, Andy Oxenham and Dr Federica Buriani, who enabled a week's testing to take place in very challenging circumstances during the COVID pandemic.

## References

Allsop, W., Bruce, T., Pearson, J. and Besley, P. (2005) 'Wave overtopping at vertical and steep seawalls', *Proceedings of the Institution of Civil Engineers – Maritime Engineering*, Vol.158, Iss.3, pp.103-114. doi: 10.1680/maen.2005.158.3.103.

Altomare, C., Laucelli, D.B., Mase, H. and Gironella, X. (2020) 'Determination of Semi-Empirical Models for Mean Wave Overtopping Using an Evolutionary Polynomial Paradigm', *Journal of Marine Science and Engineering,* 8(8), 570. doi: 10.3390/jmse8080570.

Bricheno, L.M. and Wolf, J. (2018) 'Future wave conditions of Europe, in response to high-end climate change scenarios', *Journal of Geophysical Research: Oceans*, 123, pp.8762-8791. doi: 10.1029/2018JC013866.

Chakrabarti, S. (1998) 'Physical Model Testing of Floating Offshore Structures', *Dynamic Positioning Conference,* 13 – 14 October. Available at: http://dynamic-positioning.com/proceedings/dp1998/DSubrata.PDF (Accessed: 19 April 2021).

de Rouck, J., Geeraerts, J., Troch, P., Kortenhaus, A., Pullen, T. and Franco, L. (2005) 'New Results on Scale Effects for Wave Overtopping at Coastal Structures', International Conference on Coastlines, Structures and Breakwaters 2005, January, pp. 29-43. Available at: https://www.icevirtuallibrary.com/doi/full/10.1680/csab2005hsad.34556.0003 (Accessed: 08 October 2020).

de Waal, J.P., Tönjes, P. and van der Meer, J. (1996) 'Wave Overtopping of Vertical Structures including Wind Effect, *Proceedings of the 25th International Conference on Coastal Engineering*, pp.2216-2229.

Den Bieman, J.P., Wilms, J.M., van den Boogaard, H.F.P. and van Gent, M.R.A. (2020) 'Prediction of Mean Wave Overtopping Discharge using Gradient Boosting Decision Trees', *Water*, 12, 1703. doi: 10.3390/W12061703.

Dong, S., Albofathi, S., Salauddin, M., Tan, Z.H. and Pearson, J.M. (2020) 'Enhancing climate resilience of vertical seawall with retrofitting – A physical modelling study', *Applied Ocean Research*, 103, Article: 102331. doi: 10.1016/j.apor.2020.102331.

Duarte, C.M., Ferreira, J.C. and Fortes, J. (2020) 'Risk Modelling in Urban Coastal Areas to Support Adaptation to Climate Change and Extreme Weather Events: Early Warning, Emergency Planning and Risk Management Systems', *Journal of Coastal Research*, 95(sp1), pp.785-789. doi: 10.2112/SI95-153.1.

Environment Agency (2015) *Delivering benefits through evidence – Cost estimation for coastal protection – summary of* evidence. Bristol: Environment Agency. Available at: https://assets.publishing.service.gov.uk/government/uploads/system/uploads/attachment_data/file/411178/Cost_estimation_for_coastal_protection.pdf#:~:text=Cost%20estimation%20for%20coastal%20protection%20–summary%20of%20evidence,as%20efficiently%20and%20effectively%20as%20possible.%20It%20also (Accessed: 17 December 2020).

Environment Agency (2020) Flood and Coastal Erosion Risk Management Research Programme – Updated wave overtopping and assessment manual (EurOtop) and calculation tool (Bayonet GPE). Bristol: Environment Agency. Available at: https://assets.publishing.service.gov.uk/government/uploads/system/uploads/attachment_data/file/935602/Updated_wave_overtopping_and_assessment_manual_and_calculation_tool_-_summary.pdf (Accessed: 30 December 2020).

European Commission (2020) *Integrated Coastal Management*. Available at: https://ec.europa.eu/environment/iczm/index_en.htm (Accessed: 24 November 2020).

Formentin, S.M., Zanuttigh, B. and Van der Meer, J.W. (2017) 'A Neural Network Tool for Predicting Wave Reflection, Overtopping and Transmission', *Coastal Engineering Journal*, 59, No.1, pp.1750006-1-1750006-31. doi: 10.1142/S0578563417500061.

H R Wallingford Ltd (1999) '*Wave Overtopping of Seawalls, Design and Assessment Manual, R&D Technical Report W178*'. Bristol: Environment Agency. Available at: http://www.overtopping-manual.com/assets/downloads/EA_Overtopping_Manual_w178.pdf (Accessed: 15 January 2021).

H R Wallingford Ltd (2019) *Bayonet GPE*. Available at: https://overtopping.co.uk/ (Accessed: 17 March 2021).

Horton, B.P., Khan, N.S., Cahill, N., Lee, J.S.H., Shaw, T.A., Garner, A.J., Kemp, A.C., Engelhart, S.E. and Rahmstorf, S. (2020) 'Estimating global mean sea-level

rise and its uncertainties by 2100 and 2300 from an expert survey', *npj Climate and Atmospheric Science*, 3, Article:18. doi: 10.1038/s41612-020-0121-5.

Hughes, S.A. (1993) *Physical Models and Laboratory Techniques in Coastal Engineering*. Singapore: World Scientific Publishing Company.

ITTC (2017) *Recommended Procedures and Guidelines – Laboratory Modelling of Waves: regular, irregular and extreme events.* Zurich, Switzerland: ITTC Association. Available at: https://www.ittc.info/mdeia/8095/75-02-07-012.pdf (Accessed: 20 December 2020).

Iwagaki, Y., Tsuchiya, Y. and Inoue, M. (1966) 'On the Effect of Wind on Wave Overtopping on Vertical Seawalls', *Bulletin of the Disaster Prevention Research Institute*, 16(1), pp.11-30. Available at: https://hdl.handle.net/2433/124717 (Accessed: 22 December 2020).

Jensen, O.J. and Sorensen, T. (1979) 'Overspilling/overtopping of rubble-mound breakwaters. Results of studies, useful in design procedures', *Coastal Engineering*, Vol. 3, pp. 51-65. doi: 10.1016/0378-3838(79)90005-X.

Kerpen, N.B., Daemrich, K-F., Lojek, O. and Schlurmann, T. (2020) 'Effect of Variations in Water Level and Wave Steepness on the Robustness of Wave Overtopping Estimation', *Journal of Marine Science and Engineering*, 8, 63. doi: 10.3390/jmse8020063.

Lindsey, R. (2021) *Climate Change: Global Sea Level.* Available at: https://www.climate.gov/news-features/understanding-climate/climate-change-global-sea-level (Accessed: 26 January 2021).

McDonald, G. (2019) 'Hurricane-force winds batter Devon and Cornwall as 113 mph gusts recorded', *Plymouth Live*, 2 November. Available at: https://www.plymouthherald.co.uk/hurricane-force-winds-batter-devon-3494633 (Accessed: 1 December 2020).

Murakami, K., Maki, D. and Ogino, K. (2019) 'Effect of Wind Velocity on Wave Overtopping', *Proceedings of the 10th International Conference on Asian and Pacific Coasts (APAC 2019)*, Hanoi, Vietnam: 25 – 28 September. doi: 10.1007/978-981-15-0291-0_9.

Muzik, I. and Kirby, A. (1991) 'Spray overtopping rates for Tarsiut Island – model and field-study results', *Canadian Journal of Civil Engineering*, Vol. 19, No. 3, pp. 469-477. doi: 10.1139/l92-057.

Parliamentary Office of Science & Technology (2020) *Sea Level Rise*, Postnote 363. Available at: https://www.parliament.uk/globalassets/documents/post/postpn363-sea-level-rise.pdf (Accessed: 24 November 2020).

Pearson, J., Bruce, T., Allsop, W. and Gironella, X. (2002) 'Violent wave overtopping – Measurements at large and small scale', *Proceedings of the 28th International*

*Conference on Coastal Engineering*, Vol. 3, pp. 2227-2238. doi: 10.1142/9789812791306_0187.

Pullen, T., Allsop, W., Bruce, T. and Pearson, J. (2009) 'Field and laboratory measurements of mean overtopping discharges and spatial distributions at vertical sea walls', *Coastal Engineering,* 56, Issue 2, pp.121-140. doi: 10.1016/j.coastaleng.2008.03.011.

Pullen, T., Liu, Y., Morillas, P.O. et al (2018) 'A generic and practical wave overtopping model that includes uncertainty', *Proceedings of the Institution of Civil Engineers – Maritime Engineering*, Vol.171, Iss.3, pp.109-120. doi: 10.1680/jmaen.2017.31.

Reeve, D., Chadwick, A. and Fleming, C. (2012) *Coastal Engineering Processes, Theory and Design Practice*. 2nd edn. Florida, USA: Taylor & Francis Group.

Reis, M.T., Neves, M.G. and Hedges, T. (2008) 'Investigating the length of scale models tests to determine mean wave overtopping discharges', *Coastal Engineering Journal*, Vol. 50, No. 4, pp. 441-462. doi: 10.1142/S057856340800182X.

United Nations (2017) 'Factsheet: People and Oceans', *The Ocean Conference,* United Nations, New York, 5 – 9 June. Available at: https://www.un.org/sustainabledevelopment/wp-content/uploads/2017/05/Ocean-fact-sheet-package.pdf (Accessed: 24 November 2020).

Van der Meer, J.W., Allsop, N.W.H, Bruce, T., De Rouck, J., Kortenhaus, A., Pullen, T., Schűttrumpf, H., Troch, P. and Zanuttigh, B. (2018) *EurOtop, Manual on wave overtopping of sea defences and related structures. An overtopping manual largely based on European research, but for worldwide application*. 2nd edn. Available at: http://www.overtopping-manual.com/assets/downloads/EurOtop_II_2018_Final_version.pdf (Accessed: 30 September 2020).

Van Gent, M.R.A., van den Boogaard, H.F.P., Pozueta, B. and Medina, J.R. (2007) 'Neural network modelling of wave overtopping at coastal structures', *Coastal Engineering*, Vol.54, pp.586-593. CLASH database available at: https://www.deltares.nl/en/software/overtopping-neural-network/ (Accessed: 15 January 2021).

Ward, D.L., Wibner, C., Zhang, J. and Edge, B. (1994) 'Wind Effects on Runup and Overtopping', *24th International Conference on Coastal Engineering*. Kobe, Japan: 23 - 28 October. doi: 10.1061/9780784400890.122.

Ward, D.L., Wibner, C., Zhang, J. and Cinotto, C.M. (1996) 'Wind Effects on Runup and Overtopping of Coastal Structures', *25th International Conference on Coastal Engineering*. Orlando, Florida, USA: 2 - 6 September. doi: 10.1061/9780784402429.171.

Williams, H.E., Briganti, R., Romano, A. and Dodd, N. (2019) 'Experimental Analysis of Wave Overtopping: A New Small Scale Laboratory Dataset for the Assessment of

Uncertainty for Smooth Sloped and Vertical Coastal Structures', *Journal of Marine Science and Engineering*, 7, 217. doi: 10.3390/jmse7070217.

Yamashiro, M., Yoshida, A., Hashimoto, H., Kurushima, N. and Irie, I. (2004) 'Conversion of the Wind Velocity in Wave-Overtopping Experiment into the Wind Velocity of the Real Coast', *Proceedings of Civil Engineering in the Ocean*, Vol.20, pp.653-658. doi: 10.2208/prooe.20.653.

Zanuttigh, B., Formentin, S.M. and Van der Meer, J.W. (2014) 'Advances in Modelling Wave-Structure Interaction Through Artificial Neural Networks', *Coastal Engineering Proceedings*, 1(34), p.structures.69. doi: 10.9753/ice.v34.structures.69.

Zanuttigh, B., Formentin, S.M. and Van der Meer, J.W. (2016) 'Prediction of extreme and tolerable wave overtopping discharges through an advanced neural network', *Ocean Engineering*, 127, pp.7-22. doi: 10.1016/j.oceaneng.2016.09.032.